

## Appendix H Response-Spectrum Modal Analysis of a Free-standing Intake Tower

### H-1. Introduction

*a.* The example problem presented in this appendix illustrates the response spectrum modal analysis (RSMA) procedures applied to the earthquake response computation of a free-standing intake tower. The purpose of this example is to demonstrate the structural modeling and the process of computing earthquake demands for a free-standing intake tower due to site-specific and standard response spectra.

*b.* The structural modeling including the added hydrodynamic masses of the surrounding and contained water is described. The natural periods and mode shapes are determined with and without the effect of shear deformation considered, and then used to compute tower displacements, shears, and moments induced by a standard and a site-specific ground motion. The seismic responses are computed separately for excitation along each horizontal axis of the tower and then combined to obtain the total response for combined excitation along both axes.

*c.* See paragraph H-7 for a conversion chart.

### H-2. Description of Example Tower

The example intake tower is shown in Figure H-1, where  $H_s$  is the structure height,  $H_o$  is the depth of outside water, and  $H_i$  is the depth of inside water. It is 60.96 m high with a rectangular cross section whose dimensions and wall thickness vary along the height of the tower (paragraph H-5a). The tower is built on a rock foundation, and the normal water pool is at elevation (el) 1016.81 m.

### H-3. Earthquake Ground Motion

The earthquake ground motions for the example problem consist of a site-specific and a standard response spectrum developed for a rock site in the San Francisco Bay area. The site-specific ground motion is the equal hazard response spectrum with a return period of 1000 years developed in Appendix G (Example 2). The peak ground acceleration for the site-specific ground motion is 0.7 g, representing a rock site 21 km east of the San Andreas Fault and 7 km west of the Hayward Fault, as shown in Figure G2-1. The standard response spectrum is based on the 1994 National Earthquake Hazards Reduction Program spectral acceleration maps (Building Seismic Safety Council 1994) and was developed in accord with CECW-ET memorandum, Earthquake Design Guidance for Structures, dated 30 October 1996. The estimated effective peak ground acceleration for the standard ground motion is 0.6756 g. The standard and site-specific response spectra are shown in Figure H-2.

### H-4. Method of Analysis

The example tower is analyzed using the response spectrum modal superposition method described in paragraph 2-8. The analyses are carried out using the computer program SAP-IV, but spreadsheet calculations are also provided to illustrate the analysis procedures. Slender towers with cross-section dimensions 10 times less than the height of the structure can adequately be represented solely by the flexural deformations of the tower. However, the effects of shear deformations on vibration frequencies

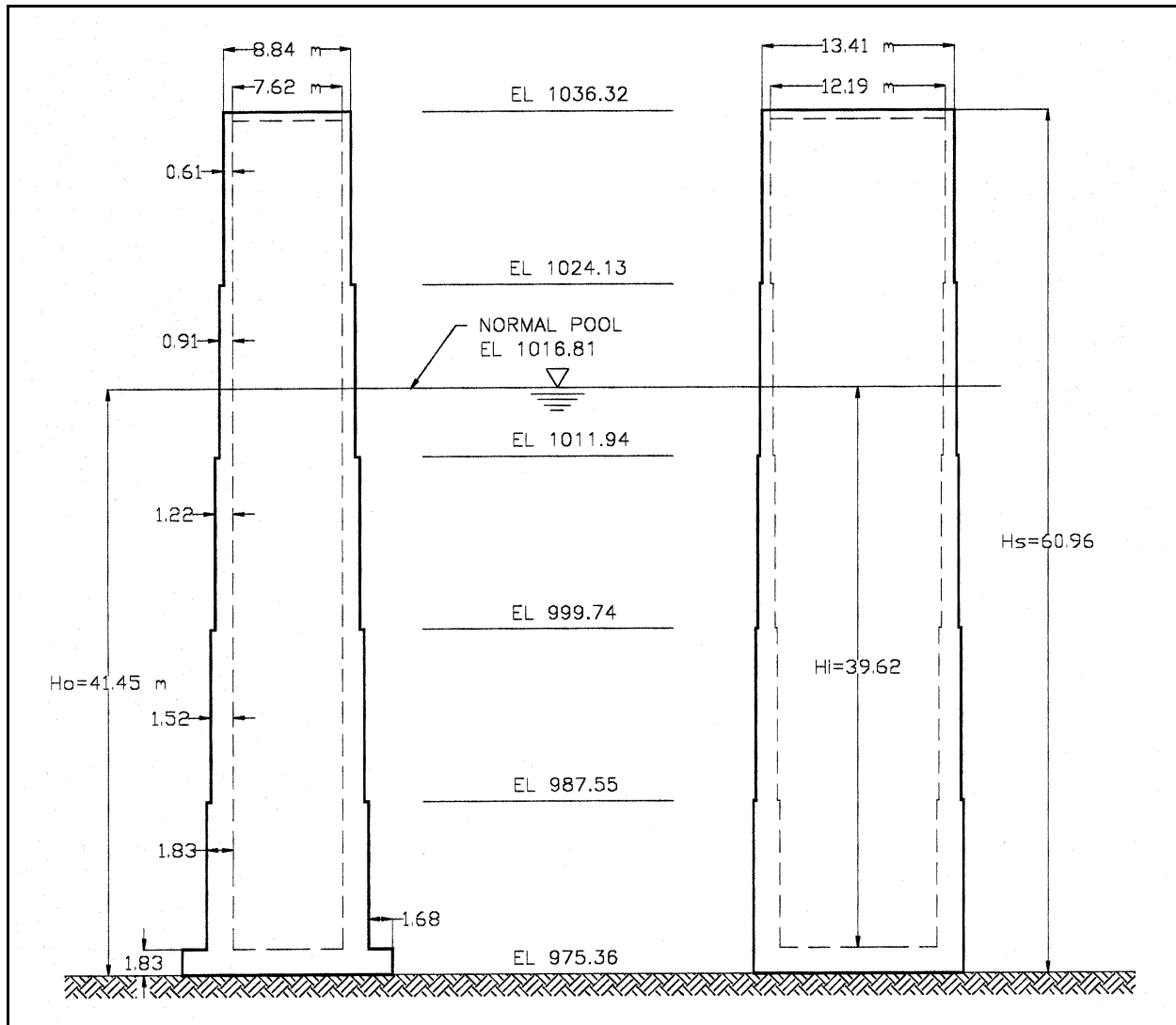


Figure H-1. Geometry of example intake tower

and section forces, especially for higher modes, are significant when the cross-section dimensions exceed 1/10 of the tower height. In this example, the computer analyses are used to demonstrate the effects of shear deformations as well as the number of vibration modes that should be included in the response analysis of the tower. The spreadsheet calculations, on the other hand, are employed to illustrate the steps involved in the customary two-mode approximation method of tower analysis.

### H-5. Structural Model

The example tower was idealized as a series of beam elements with the mass of tower lumped at the element nodal points. The idealized models for excitation along the transverse and longitudinal axes of the structure are shown in Figures H-3 and H-4, respectively. The two models are similar, except for the stiffness properties and the added mass of water, which depend on direction of the excitation. At each cross-section discontinuity, a nodal point was introduced to generate beam elements having uniform

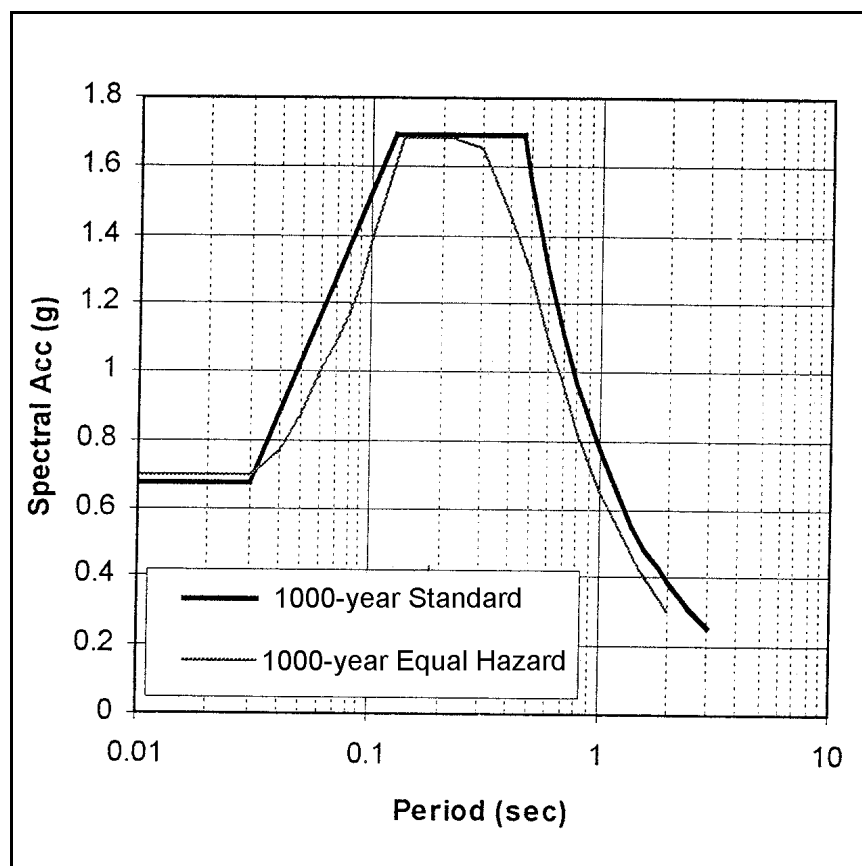


Figure H-2. Site-specific and standard response spectra for rock site in San Francisco Bay area

cross-section properties. In addition, midpoint nodes and a node at the water pool elevation were also provided for greater accuracy. Except for Node 1, which is fixed, all other nodes include one translation and one rotational degree of freedom. Each model, therefore, consists of 12 beam elements and 13 nodal points with a total of 24 degrees of freedom. The hydrodynamic interaction effects of the outside and inside water are approximated by the equivalent added hydrodynamic masses described in *b* below. The computed added masses of water are then combined with the mass of the structure in the earthquake response analysis of the tower.

*a. Structural mass and section parameters.* In the computer analysis, the element stiffness properties and lumped masses are computed from the cross-section area, mass, and moments of inertia. The cross-section properties at each level of discontinuity are computed using the dimensions provided in Figure H-1. In the following calculations  $A_{sx}$  and  $A_{sy}$  are the shear area associated with shear forces in x- and y-directions, respectively. They are needed as input parameters, if the effects of shear deformations are to be considered in the analysis.  $I_{xx}$  is the larger moment of inertia for bending in the longitudinal direction, and  $I_{yy}$  is the smaller component corresponding to bending in the transverse direction. The structure mass  $m_0$  is given in terms of mass/unit length. The calculations are shown in the following diagrams and the results are summarized in Table H-1.

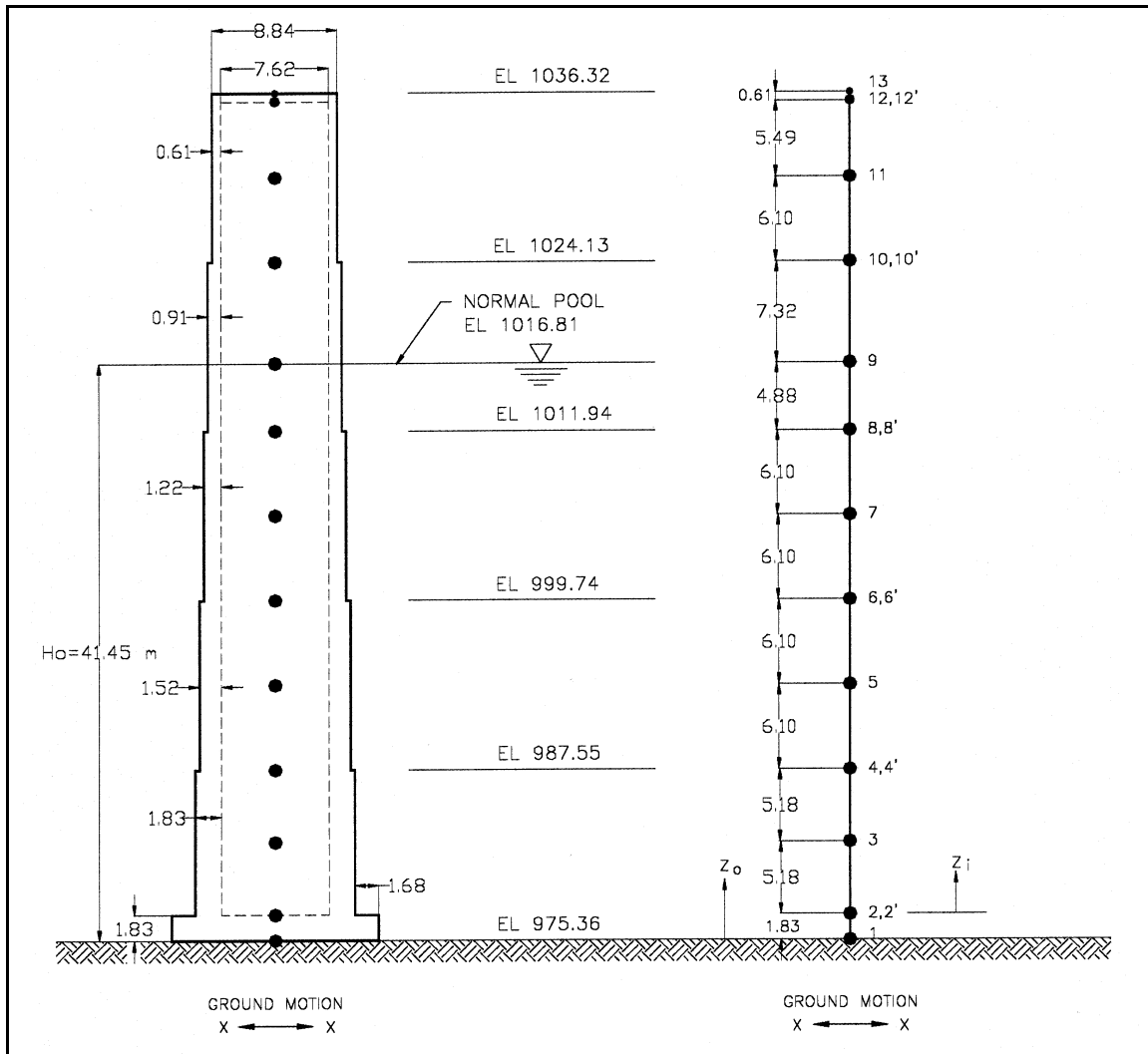
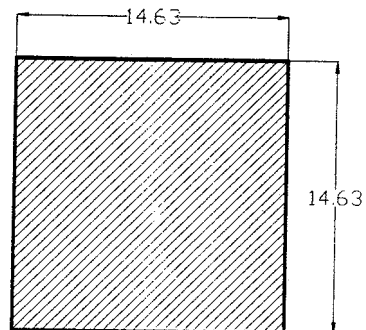


Figure H-3. Structural idealization for excitation along transverse axis (x-axis)



$EI$  975.36 – 977.19

$$A = 14.63(14.63) = 214.04 \text{ m}^2$$

$$A_{xx} = A_{yy} = 142.69 \text{ m}^2$$

$$m_o = \frac{214.04(0.024)}{9.81} = 0.524 \text{ MN} \cdot \text{sec}^2 / \text{m}^2$$

$$I_{xx} = I_{yy} = \frac{14.63(14.63)^3}{12} = 3,817.65 \text{ m}^4$$

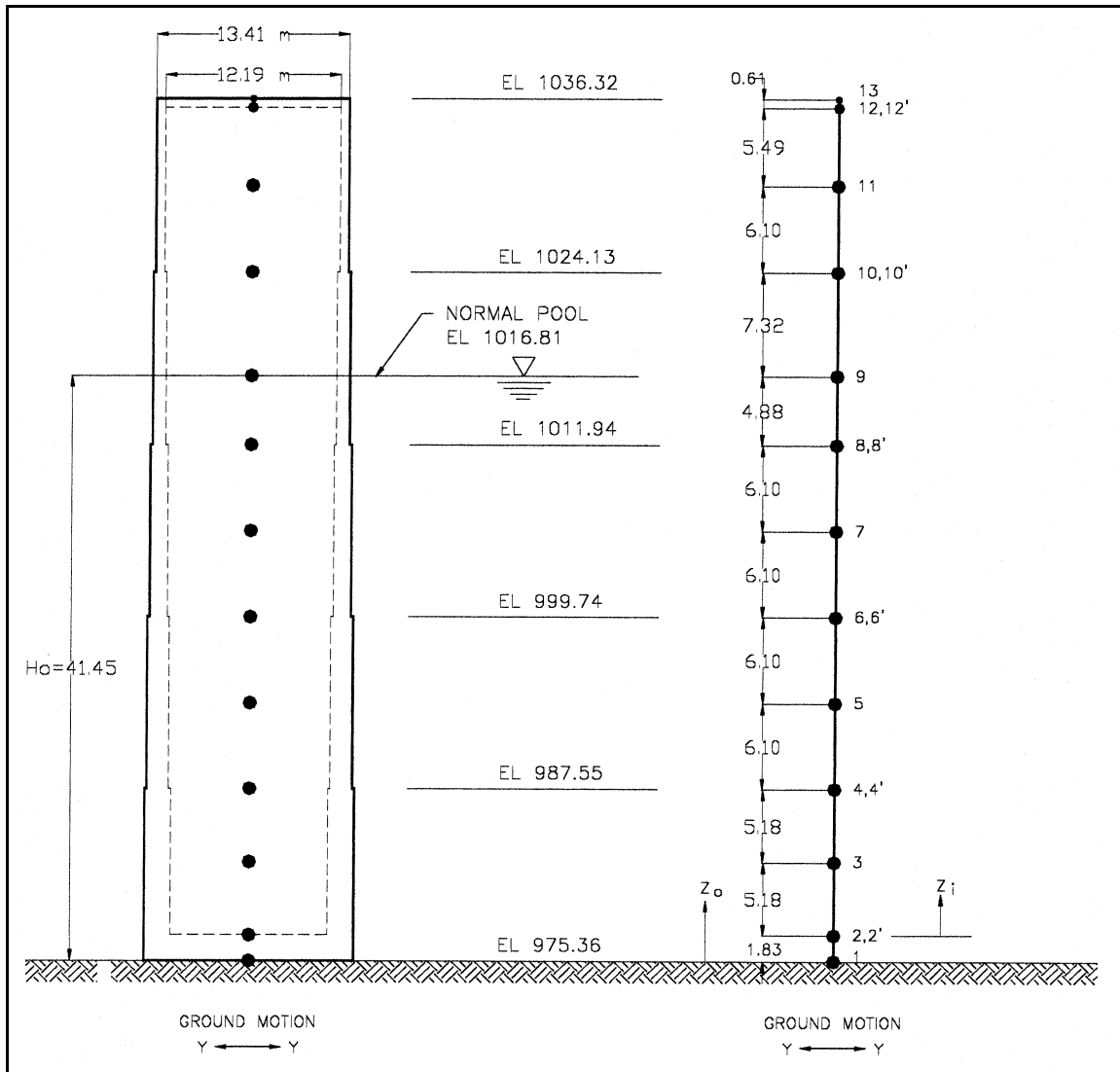
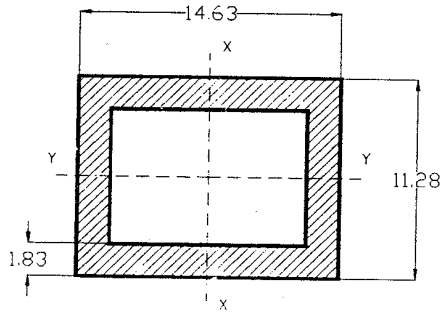


Figure H-4. Structural idealization for excitation along longitudinal axis (y-axis)

Table H-1  
Section Properties of Example Tower

| Elevation          | $A$<br>$m^2$ | $A_{sx}$<br>$m^2$ | $A_{sy}$<br>$m^2$ | $I_{xx}$<br>$m^4$ | $I_{yy}$<br>$m^4$ | $m_o$<br>$MN\text{-sec}^2/m^2$ |
|--------------------|--------------|-------------------|-------------------|-------------------|-------------------|--------------------------------|
| 975.36 to 977.19   | 214.040      | 142.69            | 142.69            | 3,817.650         | 3,817.650         | 0.524                          |
| 977.19 to 987.55   | 81.440       | 32.16             | 41.17             | 2,105.190         | 1,345.334         | 0.199                          |
| 987.55 to 999.74   | 66.698       | 25.760            | 33.926            | 1,697.202         | 1,029.647         | 0.163                          |
| 999.74 to 1011.94  | 52.802       | 19.933            | 27.050            | 1,324.208         | 762.525           | 0.129                          |
| 1011.94 to 1024.13 | 38.839       | 14.335            | 20.055            | 961.594           | 523.045           | 0.095                          |
| 1024.13 to 1035.71 | 25.657       | 9.262             | 13.393            | 626.237           | 322.521           | 0.063                          |
| 1035.71 to 1036.32 | 118.544      | 79.029            | 79.029            | 1,776.468         | 771.977           | 0.290                          |



El 977.19 - 987.55

$$A = 14.63(11.28) - 10.97(7.62) = 81.44 \text{ m}^2$$

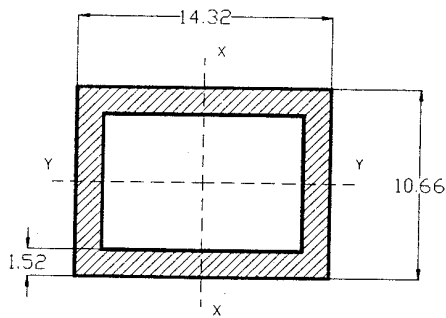
$$A_{xx} = 32.16 \text{ m}^2$$

$$A_{yy} = 41.17 \text{ m}^2$$

$$m_o = \frac{81.44(0.024)}{9.81} = 0.199 \text{ MN} - \text{sec}^2 / \text{m}^2$$

$$I_{xx} = \frac{1}{12}(11.28 \times 14.63^3 - 7.62 \times 10.97^3) = 2,105.190 \text{ m}^4$$

$$I_{yy} = \frac{1}{12}(14.63 \times 11.28^3 - 10.97 \times 7.62^3) = 1,345.334 \text{ m}^4$$



El 987.55 - 999.74

$$A = 14.32(10.66) - 11.28(7.62) = 66.698 \text{ m}^2$$

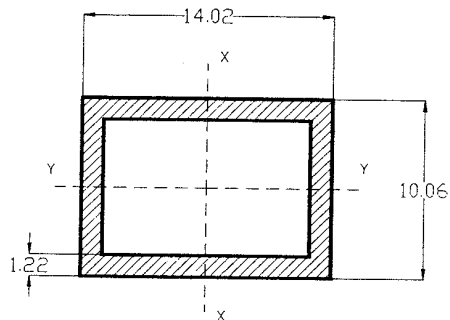
$$A_{xx} = 25.760 \text{ m}^2$$

$$A_{yy} = 33.926 \text{ m}^2$$

$$m_o = \frac{66.698(0.024)}{9.81} = 0.163 \text{ MN} - \text{sec}^2 / \text{m}^2$$

$$I_{xx} = \frac{1}{12}(10.66 \times 14.32^3 - 7.62 \times 11.28^3) = 1,697.202 \text{ m}^4$$

$$I_{yy} = \frac{1}{12}(14.32 \times 10.66^3 - 11.28 \times 7.62^3) = 1,029.647 \text{ m}^4$$



El 999.74 - 1011.94

$$A = 14.02(10.06) - 11.58(7.62) = 52.802 \text{ m}^2$$

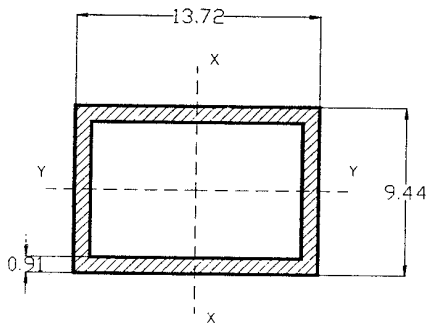
$$A_{xx} = 19.933 \text{ m}^2$$

$$A_{yy} = 27.050 \text{ m}^2$$

$$m_o = \frac{52.802(0.024)}{9.81} = 0.129 \text{ MN} - \text{sec}^2 / \text{m}^2$$

$$I_{xx} = \frac{1}{12}(10.06 \times 14.02^3 - 7.62 \times 11.58^3) = 1,324.208 \text{ m}^4$$

$$I_{yy} = \frac{1}{12}(14.02 \times 10.06^3 - 11.58 \times 7.62^3) = 762.525 \text{ m}^4$$



El 101194 - 1024.13

$$A = 13.72(9.44) - 11.9(7.62) = 38.839 \text{ m}^2$$

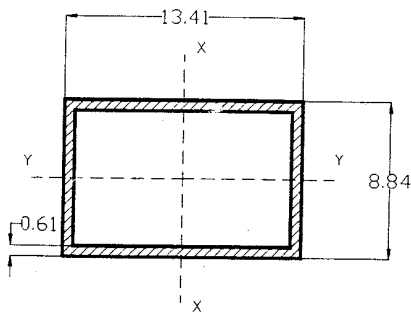
$$A_{xx} = 14.335 \text{ m}^2$$

$$A_{yy} = 20.055 \text{ m}^2$$

$$m_o = \frac{38.839(0.024)}{9.81} = 0.095 \text{ MN} \cdot \text{sec}^2 / \text{m}^2$$

$$I_{xx} = \frac{1}{12}(9.44 \times 13.72^3 - 7.62 \times 11.9^3) = 961.594 \text{ m}^4$$

$$I_{yy} = \frac{1}{12}(13.72 \times 9.44^3 - 11.9 \times 7.62^3) = 523.045 \text{ m}^4$$



El 1024.13 - 1035.71

$$A = 13.41(8.84) - 12.19(7.62) = 25.657 \text{ m}^2$$

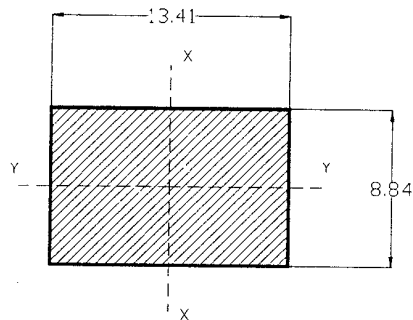
$$A_{xx} = 9.262 \text{ m}^2$$

$$A_{yy} = 13.393 \text{ m}^2$$

$$m_o = \frac{25.657(0.024)}{9.81} = 0.063 \text{ MN} \cdot \text{sec}^2 / \text{m}^2$$

$$I_{xx} = \frac{1}{12}(8.84 \times 13.41^3 - 7.62 \times 12.19^3) = 626.237 \text{ m}^4$$

$$I_{yy} = \frac{1}{12}(13.41 \times 8.84^3 - 12.19 \times 7.62^3) = 322.521 \text{ m}^4$$



El 1035.71 - 1036.32

$$A = 13.41(8.84) = 118.544 \text{ m}^2$$

$$A_{xx} = A_{yy} = 79.029 \text{ m}^2$$

$$m_o = \frac{118.544(0.024)}{9.81} = 0.290 \text{ MN} \cdot \text{sec}^2 / \text{m}^2$$

$$I_{xx} = \frac{1}{12}(8.84 \times 13.41^3) = 1,776.468 \text{ m}^4$$

$$I_{yy} = \frac{1}{12}(13.41 \times 8.84^3) = 771.977 \text{ m}^4$$

*b. Added hydrodynamic mass.* The hydrodynamic interaction effects of the surrounding and contained water in the analysis of the example tower are approximated by an equivalent added mass of water. This concept assumes the water is incompressible, and provides added hydrodynamic mass functions that represent the inertial effects of water interacting with the tower. The computation of the added hydrodynamic mass is further simplified by the assumption of a rigid tower subjected to unit horizontal ground acceleration. In this example the added hydrodynamic mass functions for the surrounding and contained water are computed using a simplified procedure developed by Goyal and Chopra (1989). The Goyal and Chopra simplified procedure is based on the analytical solutions available for circular cylindrical towers and uniform elliptical towers. The procedure is applicable to the added hydrodynamic mass analysis of both uniform and nonuniform towers of arbitrary cross section with two axes of symmetry. For a tower of arbitrary cross section the added mass analysis is carried out, first by evaluating an “equivalent” uniform elliptical cross section, and then a corresponding “equivalent” circular cylindrical tower for which the analytical solution is available. A summary of Goyal and Chopra’s findings and assumptions, which led to their formulation of the simplified procedure, is as follows:

(1) For an infinitely long uniform tower with the same circular cross section, the added mass per unit height is

$$m_{\infty}^o = \rho_w \pi r_o^2 \quad (\text{H-1})$$

where  $\rho_w$  is the mass density of water. This is equal to the mass of the water displaced by the (solid) tower per unit height.

(2) The normalized added mass ( $m_a^o(z)/m_{\infty}^o$ ) is influenced by the slenderness ratio ( $H_o/a_o$ ), the ratio ( $a_o/b_o$ ) of the cross-sectional dimensions, the cross-sectional area  $A_o$ , and the cross-sectional shapes.

(3) The added mass per unit length of an infinitely long uniform tower is two-dimensional in the cross sectional plane of the tower and can be obtained using semianalytical procedures. This led to computation of the added mass per unit length for infinitely long uniform towers with a variety of cross sections.

(4) The computation from Step 3 indicated that the normalized added mass for uniform tower of arbitrary cross section is essentially the same as that for an “equivalent” elliptical tower. This finding led to the conclusion that the normalized added mass for a uniform tower of arbitrary cross section can therefore be obtained from the solution available for an equivalent elliptical tower. The cross-section dimensions ratio  $\tilde{a}_o/\tilde{b}_o$  and the slenderness ratio  $H_o/\tilde{a}_o$  of the equivalent elliptical tower are related to  $a_o/b_o$ ,  $A_o$ , and  $H_o$  for the actual tower by:

$$\frac{H_o}{\tilde{a}_o} = \frac{H_o}{\sqrt{A_o/\pi}} \cdot \sqrt{\frac{b_o}{a_o}} \quad (\text{H-2})$$

$$\frac{\tilde{a}_o}{\tilde{b}_o} = \frac{a_o}{b_o} \quad (\text{H-3})$$

(5) The computation of added mass for elliptical towers, however, requires a large number of graphs and tables in order to cover a wide range of cross-section parameters. To further simplify the solution

process for practical application, the uniform elliptical tower is replaced by an “equivalent” circular cylindrical tower for which a single chart or table will suffice. The slenderness ratio of the “equivalent” circular cylindrical tower is obtained from the slenderness ratio and the ratio of the corresponding elliptical cross-section dimensions.

(6) The procedure is extended to the added mass analysis of nonuniform towers, simply by applying these steps to various portions of the tower that actually are, or assumed to be, uniform.

*c. Added hydrodynamic mass of outside water for excitation along longitudinal axis.* The added hydrodynamic mass for the outside water is computed separately for excitation along the longitudinal (y) and transverse (x) axes of the tower. The rectangular tower has an outside cross-section area  $A_o(z)$ , a width of  $2a_o(z)$  perpendicular to the direction of excitation, and a dimension of  $2b_o(z)$  parallel to the direction of excitation. The following steps illustrate the computation of the added mass for the outside water for excitation along the longitudinal axis:

(1) Select Nodes 1 to 9 along the tower height for computation of added mass  $m_a^o(z)$ . At the points of discontinuity designate two nodes, one corresponding to the section above and another to the section below. For example Nodes 8 and 8' are used to account for the section changes at el 1012 m. Compute the height coordinate  $Z_o$ , section parameters  $a_o/b_o$ ,  $a_o/H_o$ , and  $A_o$  for the selected nodes, as shown in columns 2 to 5 of Table H-2.

(2) Use Equation H-2 and the actual section parameters obtained in Step 1 to determine the ratio of the cross-section dimensions  $\tilde{a}_o/\tilde{b}_o$  and the slenderness ratio  $\tilde{a}_o/H_o$  for the equivalent elliptical tower (columns 6 and 7 of Table H-2).

(3) From Figure H-5 and the section properties of the equivalent elliptical tower obtained in Step 2, determine the slenderness ratio  $\tilde{r}_o/H_o$  of the equivalent circular tower at the selected nodal point (Column 8 of Table H-2).

(4) Use Figure H-6 and section properties obtained in Step 3 to evaluate the normalized added hydrodynamic mass  $m_a^o(z)/m_\infty^o$  for the circular cylindrical towers associated with the surrounding water (Column 10 of Table H-2).

(5) Use Table 8.1 of Goyal and Chopra (1989) to compute the added hydrodynamic mass  $m_\infty^o(z)$  for an infinitely long tower with its cross section same as that of the actual tower (Column 13 of Table H-2).

(6) Determine the added hydrodynamic mass  $m_a^o(z)$  for the actual tower at the location  $z$  by multiplying the normalized added mass obtained in Step 4 by  $m_\infty^o(z)$  computed in Step 5.

(7) Repeat steps 2 to 6 for all selected nodes along the height of the tower.

*d. Added hydrodynamic mass of inside water for excitation along longitudinal axis.* The added hydrodynamic mass for the inside water is computed in a manner similar to that described for the outside water. For the example rectangular tower having inside cross sections  $A_i(z)$ , width  $2a_i(z)$  perpendicular to the direction of excitation, and dimension  $2b_i(z)$  parallel to the direction of excitation, the computation of added mass for ground motion along the longitudinal axis of the tower is as follows:

(1) Select Nodes 2 to 9 along the tower height for computation of inside added mass  $m_i^o(z)$ . Compute the height coordinate  $Z_i$ , section parameter  $a_i/b_i$ ,  $a_i/H_i$ , and  $A_i$  for the selected nodes, as shown in columns 2 to 5 of Table H-3.

**Table H-2**  
**Computation of Added Mass for the Outside Water Due to Ground Motion Along Longitudinal Axis (Y)**

| Node No. | $Z_o$<br>m | Outside Geometry  |                   |                         | Equivalent Ellipse                |                           | Equivalent Cylinder       |                   |                               | Infinitely Long Tower                               |                                 |                                                     |                                                   |
|----------|------------|-------------------|-------------------|-------------------------|-----------------------------------|---------------------------|---------------------------|-------------------|-------------------------------|-----------------------------------------------------|---------------------------------|-----------------------------------------------------|---------------------------------------------------|
|          |            | $\frac{a_o}{b_o}$ | $\frac{a_o}{H_o}$ | $A_o$<br>m <sup>2</sup> | $\frac{\tilde{a}_o}{\tilde{b}_o}$ | $\frac{\tilde{a}_o}{H_o}$ | $\frac{\tilde{r}_o}{H_o}$ | $\frac{Z_o}{H_o}$ | $\frac{m_a^o(z)}{m_\infty^o}$ | $\rho_w A_o$<br>MN-sec <sup>2</sup> /m <sup>2</sup> | $\frac{m_\infty^o}{\rho_w A_o}$ | $m_\infty^o$<br>MN-sec <sup>2</sup> /m <sup>2</sup> | $m_a^o(z)$<br>MN-sec <sup>2</sup> /m <sup>2</sup> |
| 1        | 2          | 3                 | 4                 | 5                       | 6                                 | 7                         | 8                         | 9                 | 10                            | 11                                                  | 12                              | 13                                                  | 14                                                |
| 1        | 0          | 1                 | 0.176             | 214.037                 | 1                                 | 0.199                     | 0.199                     | 0                 | 0.93                          | 0.218                                               | 1.186                           | 0.259                                               | 0.241                                             |
| 2        | 1.83       | 1                 | 0.176             | 214.037                 | 1                                 | 0.199                     | 0.199                     | 0.044             | 0.93                          | 0.218                                               | 1.186                           | 0.259                                               | 0.241                                             |
| 2'       | 1.83       | 0.771             | 0.136             | 165.026                 | 0.771                             | 0.154                     | 0.175                     | 0.044             | 0.944                         | 0.168                                               | 0.957                           | 0.161                                               | 0.152                                             |
| 3        | 7.01       | 0.771             | 0.136             | 165.026                 | 0.771                             | 0.154                     | 0.175                     | 0.169             | 0.941                         | 0.168                                               | 0.957                           | 0.161                                               | 0.152                                             |
| 4        | 12.19      | 0.771             | 0.136             | 165.026                 | 0.771                             | 0.154                     | 0.175                     | 0.294             | 0.931                         | 0.168                                               | 0.957                           | 0.161                                               | 0.150                                             |
| 4'       | 12.19      | 0.745             | 0.129             | 152.651                 | 0.745                             | 0.145                     | 0.167                     | 0.294             | 0.936                         | 0.156                                               | 0.931                           | 0.145                                               | 0.136                                             |
| 5        | 18.29      | 0.745             | 0.129             | 152.651                 | 0.745                             | 0.145                     | 0.167                     | 0.441             | 0.916                         | 0.156                                               | 0.931                           | 0.145                                               | 0.133                                             |
| 6        | 24.38      | 0.745             | 0.129             | 152.651                 | 0.745                             | 0.145                     | 0.167                     | 0.588             | 0.878                         | 0.156                                               | 0.931                           | 0.145                                               | 0.127                                             |
| 6'       | 24.38      | 0.717             | 0.121             | 141.041                 | 0.717                             | 0.137                     | 0.16                      | 0.588             | 0.885                         | 0.144                                               | 0.903                           | 0.130                                               | 0.115                                             |
| 7        | 30.48      | 0.717             | 0.121             | 141.041                 | 0.717                             | 0.137                     | 0.16                      | 0.735             | 0.808                         | 0.144                                               | 0.903                           | 0.130                                               | 0.105                                             |
| 8        | 36.58      | 0.717             | 0.121             | 141.041                 | 0.717                             | 0.137                     | 0.16                      | 0.882             | 0.615                         | 0.144                                               | 0.903                           | 0.130                                               | 0.080                                             |
| 8'       | 36.58      | 0.689             | 0.114             | 129.517                 | 0.689                             | 0.129                     | 0.153                     | 0.882             | 0.626                         | 0.132                                               | 0.875                           | 0.116                                               | 0.073                                             |
| 9        | 41.45      | 0.689             | 0.114             | 129.517                 | 0.689                             | 0.129                     | 0.153                     | 1                 | 0                             | 0.132                                               | 0.875                           | 0.116                                               | 0.000                                             |

Note:

$$\frac{\tilde{a}_o}{H_o} = \frac{1}{H_o} \sqrt{\frac{A_o}{\pi} \left( \frac{a_o}{b_o} \right)}$$

(2) Use equation given in Table H-3 and the actual section parameters obtained in Step 1 to determine the ratio of the cross-section dimensions  $\tilde{a}_i/\tilde{b}_i$  and the slenderness ratio  $\tilde{a}_i/H_i$  for the equivalent elliptical tower (columns 6 and 7 of Table H-3).

(3) From Figure H-7 and the section properties of the equivalent elliptical tower obtained in Step 2, determine the slenderness ratio  $\tilde{r}_i/H_i$  of the equivalent circular tower at the selected nodal point (Column 8 of Table H-3).

(4) Use Figure H-8 and section properties obtained in Step 3 to evaluate the normalized added hydrodynamic mass  $m_a^i(z)/m_\infty^i$  for the circular cylindrical towers associated with the inside water (Column 10 of Table H-3).

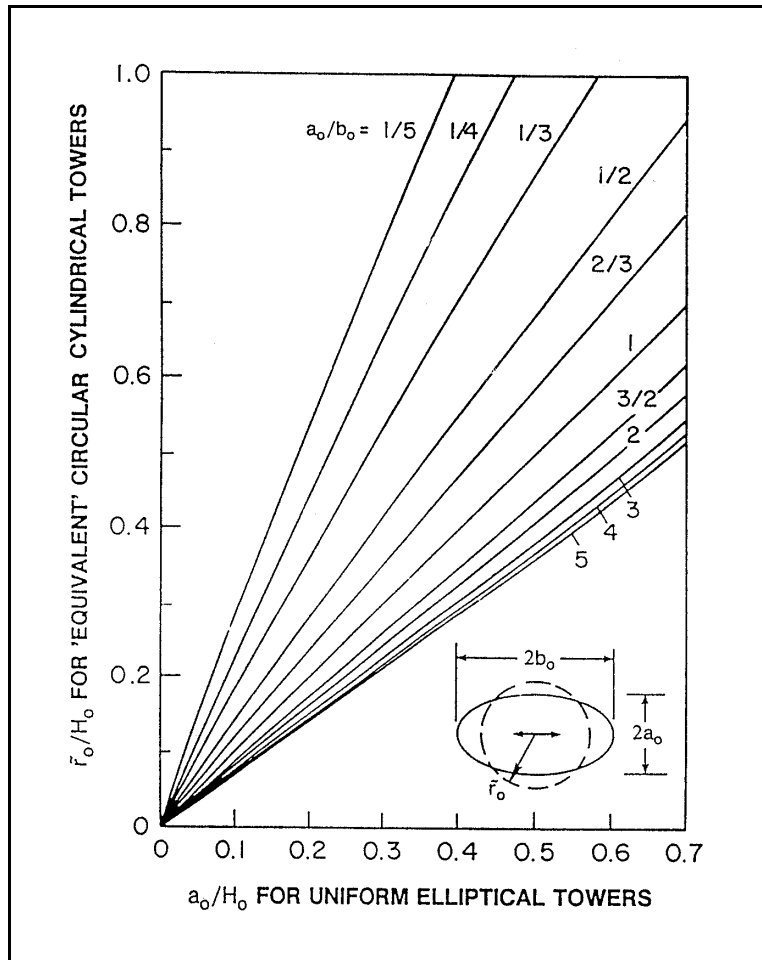


**Figure H-5. Properties of “equivalent” circular cylindrical towers for uniform elliptical towers associated with added hydrodynamic mass due to surrounding water (Goyal and Chopra 1989, courtesy of Earthquake Engineering Research Center, University of California, Berkeley)**

(5) Determine the added hydrodynamic mass  $m_a^i(z)$  for the actual tower at the location  $z$  by multiplying the normalized added mass obtained in Step 4 by  $m_\infty^i(z) = \rho_w A_i$ .

(6) Repeat steps 2 to 5 for all selected nodes along the height of the tower.

*e. Added hydrodynamic mass of outside water for excitation along transverse axis.* The added hydrodynamic mass for the outside water for excitation along the transverse direction ( $x$ -axis) is computed similar to that described for excitation along the longitudinal direction, except that  $a_o$  and  $b_o$  used previously are switched so that the dimension  $2a_o$  remains perpendicular to the direction of excitation. The results are given in Table H-4.

*f. Added hydrodynamic mass of inside water for excitation along transverse axis.* The added hydrodynamic mass for the inside water for excitation along the transverse direction ( $x$ -axis) is computed similar to that described for excitation along the longitudinal direction, except that  $a_i$  and  $b_i$  used

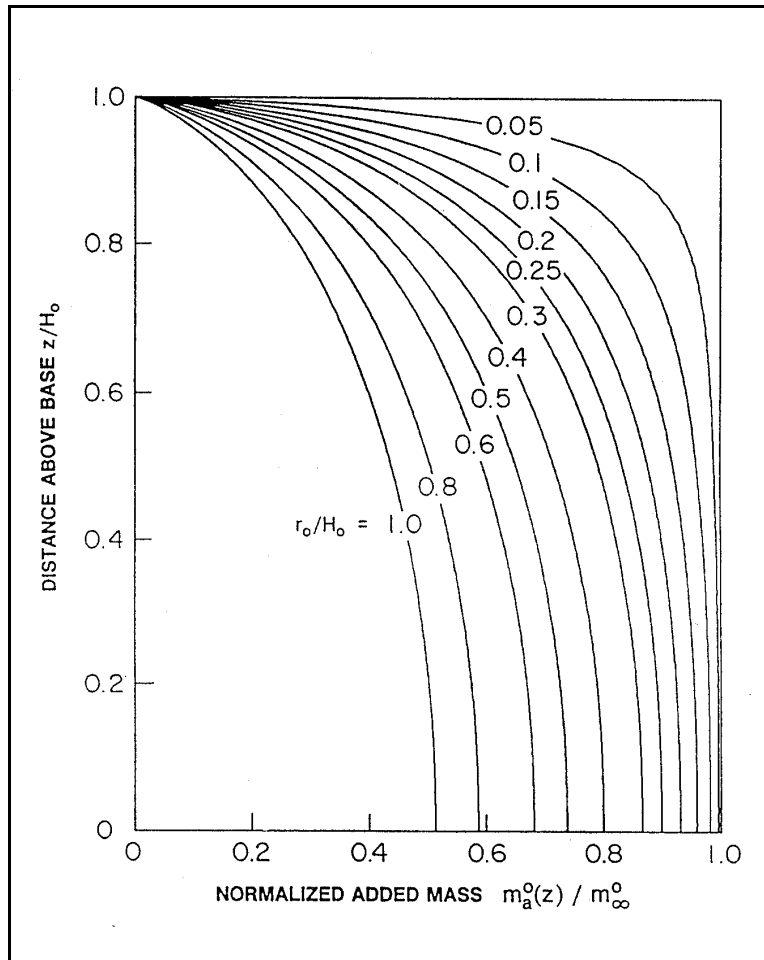


**Figure H-6. Normalized added hydrodynamic mass for circular cylindrical towers associated with surrounding water (Goyal and Chopra 1989, courtesy of Earthquake Engineering Research Center, University of California, Berkeley)**

previously are switched so that the dimension  $2a_i$  remains perpendicular to the direction of excitation. The results are given in Table H-5.

*g. Total lumped mass.* The added mass per unit length of the tower  $m_o$ , outside water  $m_a^o$ , and the inside water  $m_a^i$  for excitation along the longitudinal and transverse directions are summarized in Tables H-6 and H-7, respectively. The summation of these gives the total effective mass per foot of tower, and when multiplied by the appropriate section length provides the total lumped mass at each nodal point. Note that at the point of discontinuity the mass associated with the upper and lower sections was computed separately and then combined to obtain the total mass at that location, as shown in the last column of the tables.

**Table H-3**  
**Computation of Added Mass for the Inside Water Due to Ground Motion Along Longitudinal Axis (Y-axis)**

| Node No. | Z <sub>i</sub><br>m | Outside Geometry  |                   |                                  | Equivalent Ellipse                |                                   | Equivalent Cylinder       |                   |                               | m <sub>∞</sub> <sup>i</sup> = ρ <sub>w</sub> A <sub>i</sub><br>MN-sec <sup>2</sup> /m <sup>2</sup> | m <sub>a</sub> <sup>i</sup> (z)<br>MN-sec <sup>2</sup> /m <sup>2</sup> |
|----------|---------------------|-------------------|-------------------|----------------------------------|-----------------------------------|-----------------------------------|---------------------------|-------------------|-------------------------------|----------------------------------------------------------------------------------------------------|------------------------------------------------------------------------|
|          |                     | $\frac{a_i}{b_i}$ | $\frac{a_i}{H_i}$ | A <sub>i</sub><br>M <sup>2</sup> | $\frac{\tilde{a}_i}{\tilde{b}_i}$ | $\frac{\tilde{a}_i}{\tilde{H}_i}$ | $\frac{\tilde{r}_i}{H_i}$ | $\frac{Z_i}{H_i}$ | $\frac{m_a^i(z)}{m_\infty^i}$ |                                                                                                    |                                                                        |
| 1        | 2                   | 3                 | 4                 | 5                                | 6                                 | 7                                 | 8                         | 9                 | 10                            | 11                                                                                                 | 12                                                                     |
| 2        | 0                   | 0.694             | 0.096             | 83.59                            | 0.694                             | 0.108                             | 0.156                     | 0.0               | 1                             | 0.085                                                                                              | 0.085                                                                  |
| 3        | 5.18                | 0.694             | 0.096             | 83.59                            | 0.694                             | 0.108                             | 0.156                     | 0.131             | 1                             | 0.085                                                                                              | 0.085                                                                  |
| 4        | 10.97               | 0.694             | 0.096             | 83.59                            | 0.694                             | 0.108                             | 0.156                     | 0.277             | 1                             | 0.085                                                                                              | 0.085                                                                  |
| 4'       | 10.97               | 0.676             | 0.096             | 85.95                            | 0.676                             | 0.109                             | 0.161                     | 0.277             | 1                             | 0.088                                                                                              | 0.088                                                                  |
| 5        | 16.46               | 0.676             | 0.096             | 85.95                            | 0.676                             | 0.109                             | 0.161                     | 0.415             | 0.998                         | 0.088                                                                                              | 0.088                                                                  |
| 6        | 22.56               | 0.676             | 0.096             | 85.95                            | 0.676                             | 0.109                             | 0.161                     | 0.569             | 0.993                         | 0.088                                                                                              | 0.087                                                                  |
| 6'       | 22.56               | 0.658             | 0.096             | 88.24                            | 0.658                             | 0.109                             | 0.165                     | 0.569             | 0.992                         | 0.090                                                                                              | 0.089                                                                  |
| 7        | 28.65               | 0.658             | 0.096             | 88.24                            | 0.658                             | 0.109                             | 0.165                     | 0.723             | 0.961                         | 0.090                                                                                              | 0.086                                                                  |
| 8        | 34.75               | 0.658             | 0.096             | 88.24                            | 0.658                             | 0.109                             | 0.165                     | 0.877             | 0.787                         | 0.090                                                                                              | 0.071                                                                  |
| 8'       | 34.75               | 0.641             | 0.096             | 90.68                            | 0.641                             | 0.109                             | 0.169                     | 0.877             | 0.780                         | 0.092                                                                                              | 0.072                                                                  |
| 9        | 39.62               | 0.641             | 0.096             | 90.68                            | 0.641                             | 0.109                             | 0.169                     | 1                 | 0                             | 0.092                                                                                              | 0.000                                                                  |

Note:

$$\frac{\tilde{a}_i}{\tilde{H}_i} = \frac{1}{H_i} \sqrt{\frac{A_i}{\pi} \left( \frac{a_i}{b_i} \right)}$$

## H-6. Computation of Earthquake Response

Computation of earthquake response of the example tower consists of evaluating the following:

- a. The natural periods and mode shapes along the transverse and longitudinal axes.
- b. The maximum deflections, shears, and moments due to transverse excitation.
- c. The maximum deflections, shears, and moments due to longitudinal excitation.
- d. The total response by combining the transverse and longitudinal responses.

The earthquake response of the tower is computed using both the two-mode approximation method carried out by spreadsheet and the computer analysis including 10 modes of vibration. The two-mode approximation method uses the site-specific spectra as the seismic input, whereas both the site-specific and standard spectra are employed in the computer analysis.

- a. *Frequencies and mode shapes.*

(1) The natural periods and mode shapes of the example tower were determined using the structural model and the total lumped masses developed in paragraph H-5. The analyses were performed for two cases, with and without the effect of shear deformations. The results for the 10 lowest periods of

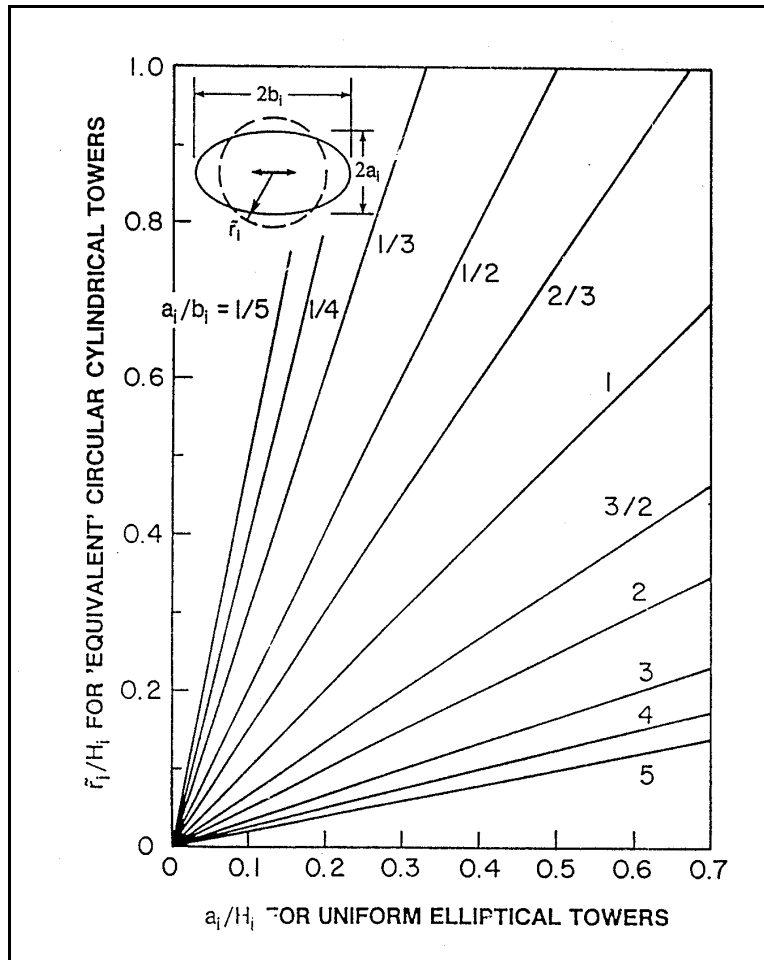


**Figure H-7. Properties of "equivalent" circular cylindrical towers for uniform elliptical towers associated with added hydrodynamic mass due to inside water (Goyal and Chopra 1989, courtesy of Earthquake Engineering Research Center, University of California, Berkeley)**

vibration along the longitudinal and transverse axes of the tower are summarized in Table H-8. The results show that the shear deformation increases periods of vibration of the example tower by about 10 to 40 percent for the first and second modes, 80 percent for the third mode, and as high as 2.5 to 3 times for the fifth mode. This rather significant effect is not all that surprising, considering that the average slenderness ratio of the example tower is about 16.5 percent in the transverse and 23 percent in the longitudinal direction. The effect of shear deformation can be neglected only if the slenderness ratio is less than 10 percent. The results also show that the effect of shear deformation is most significant in the higher modes where the vibration wavelength approaches the section dimensions of the tower. The normalized mode shapes for the lowest five modes of vibration are displayed in Figure H-9. Each mode shape was normalized to have a maximum value of unity.

(2) Alternatively, the periods and mode shapes for the first two modes may be obtained using the approximate method described in EM 1110-2-2400. In this example, however, the periods and mode shapes computed by the computer program SAP-IV will be used in the approximate two-mode analysis described in the subsequent sections.

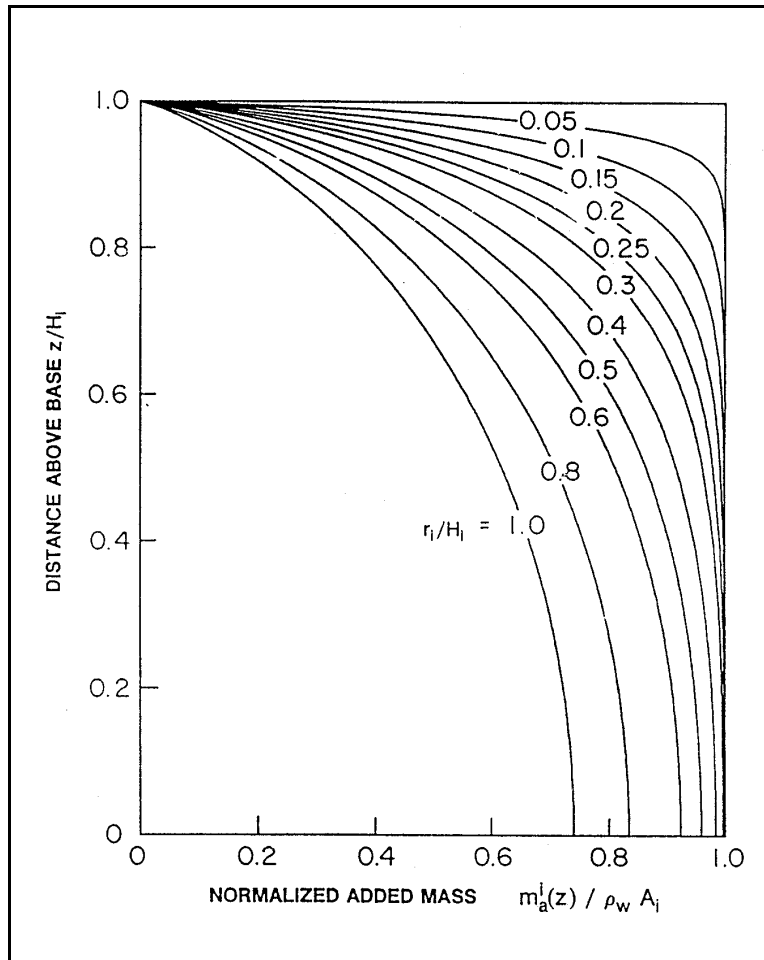


**Figure H-8. Normalized added hydrodynamic mass for circular cylindrical towers associated with inside water (Goyal and Chopra 1989, courtesy of Earthquake Engineering Research Center, University of California, Berkeley)**

*b. Response due to transverse excitation.*

(1) Two-mode approximation. The two-mode approximation of the tower response due to the site-specific ground motion along the transverse axis  $x$  is illustrated in Tables H-9 to H-11. The Mode-1 and Mode-2 responses are given in Tables H-9 and H-10, respectively, and the total response due to both modes are shown in Table H-11. The computation for Mode-1 response is as follows:

(a) The circular frequency  $\omega_1$  is obtained from Table H-8 using:

$$\omega_1 = \frac{2\pi}{T} = 2(3.1416)/(0.504) = 12.467 \text{ rad/sec} \quad (\text{H-4})$$

(b) The spectral acceleration  $S_{a1}(T_1, \xi_1) = 1.289 g$  for  $T_1 = 0.504$  sec and  $\xi_1 = 5$  percent is obtained from the site-specific response spectrum in Figure H-2.

Table H-4  
Computation of Added Mass for the Outside Water Due to Ground Motion Along Transverse Direction (x-axis)

| Node No. | $Z_o$<br>m | Outside Geometry  |                   |                         | Equivalent Ellipse                |                                   | Equivalent Cylinder       |                   |                          | Infinitely Long Tower                               |                            |                                                |                                                   |
|----------|------------|-------------------|-------------------|-------------------------|-----------------------------------|-----------------------------------|---------------------------|-------------------|--------------------------|-----------------------------------------------------|----------------------------|------------------------------------------------|---------------------------------------------------|
|          |            | $\frac{a_o}{b_o}$ | $\frac{a_o}{H_o}$ | $A_o$<br>m <sup>2</sup> | $\frac{\tilde{a}_o}{\tilde{b}_o}$ | $\frac{\tilde{a}_o}{\tilde{H}_o}$ | $\frac{\tilde{r}_o}{H_o}$ | $\frac{Z_o}{H_o}$ | $\frac{m_a^o(z)}{m_w^o}$ | $\rho_w A_o$<br>MN-sec <sup>2</sup> /m <sup>2</sup> | $\frac{m_w^o}{\rho_w A_o}$ | $m_w^o$<br>MN-sec <sup>2</sup> /m <sup>2</sup> | $m_a^o(z)$<br>MN-sec <sup>2</sup> /m <sup>2</sup> |
| 1        | 2          | 3                 | 4                 | 5                       | 6                                 | 7                                 | 8                         | 9                 | 10                       | 11                                                  | 12                         | 13                                             | 14                                                |
| 1        | 0          | 1                 | 0.176             | 214.037                 | 1                                 | 0.199                             | 0.199                     | 0                 | 0.931                    | 0.218                                               | 1.186                      | 0.259                                          | 0.241                                             |
| 2        | 1.83       | 1                 | 0.176             | 214.037                 | 1                                 | 0.199                             | 0.199                     | 0.044             | 0.931                    | 0.218                                               | 1.186                      | 0.259                                          | 0.241                                             |
| 2'       | 1.83       | 1.297             | 0.176             | 165.026                 | 1.297                             | 0.199                             | 0.184                     | 0.044             | 0.939                    | 0.168                                               | 1.468                      | 0.247                                          | 0.232                                             |
| 3        | 7.01       | 1.297             | 0.176             | 165.026                 | 1.297                             | 0.199                             | 0.184                     | 0.169             | 0.935                    | 0.168                                               | 1.468                      | 0.247                                          | 0.231                                             |
| 4        | 12.19      | 1.297             | 0.176             | 165.026                 | 1.297                             | 0.199                             | 0.184                     | 0.294             | 0.925                    | 0.168                                               | 1.468                      | 0.247                                          | 0.228                                             |
| 4'       | 12.19      | 1.343             | 0.173             | 152.651                 | 1.343                             | 0.195                             | 0.179                     | 0.294             | 0.928                    | 0.156                                               | 1.512                      | 0.236                                          | 0.219                                             |
| 5        | 18.29      | 1.343             | 0.173             | 152.651                 | 1.343                             | 0.195                             | 0.179                     | 0.441             | 0.907                    | 0.156                                               | 1.512                      | 0.236                                          | 0.214                                             |
| 6        | 24.38      | 1.343             | 0.173             | 152.651                 | 1.343                             | 0.195                             | 0.179                     | 0.588             | 0.866                    | 0.156                                               | 1.512                      | 0.236                                          | 0.204                                             |
| 6'       | 24.38      | 1.394             | 0.169             | 141.041                 | 1.394                             | 0.191                             | 0.172                     | 0.588             | 0.873                    | 0.144                                               | 1.560                      | 0.225                                          | 0.196                                             |
| 7        | 30.48      | 1.394             | 0.169             | 141.041                 | 1.394                             | 0.191                             | 0.172                     | 0.735             | 0.798                    | 0.144                                               | 1.560                      | 0.225                                          | 0.180                                             |
| 8        | 36.58      | 1.394             | 0.169             | 141.041                 | 1.394                             | 0.191                             | 0.172                     | 0.882             | 0.597                    | 0.144                                               | 1.560                      | 0.225                                          | 0.134                                             |
| 8'       | 36.58      | 1.452             | 0.165             | 129.517                 | 1.452                             | 0.187                             | 0.166                     | 0.882             | 0.606                    | 0.132                                               | 1.615                      | 0.213                                          | 0.129                                             |
| 9        | 41.45      | 1.452             | 0.165             | 129.517                 | 1.452                             | 0.187                             | 0.166                     | 1                 | 0                        | 0.132                                               | 1.615                      | 0.213                                          | 0.000                                             |

Note:

$$\frac{\tilde{a}_o}{H_o} = \frac{1}{H_o} \sqrt{\frac{A_o}{\pi} \left( \frac{a_o}{b_o} \right)}$$

(c) The normalized mode shape  $\phi_{jl}$  in Column 2 of Table H-9 was determined by the computer program SAP-IV, as described in the previous paragraph. Here the subscript  $j$  refers to nodal points along the tower height, and subscript  $l$  is the mode number.

(d) The nodal mass  $m_j$  in Column 3 is the combined structural and outside and inside mass of water for excitation in the transverse direction (Table H-7).

(e) The modal earthquake-excitation factor  $L_1 = \sum m_j \phi_{j1} = 4.134$  is obtained by multiplying Column 2 by Column 3 and summing the results for all nodes.

(f) The modal mass  $M_1 = \sum m_j \phi_{j1}^2 = 1.874$  is computed by multiplying Column 2 by Column 4 and summing the results for all nodes.

(g) When  $L_1$  and  $M_1$  are known, the modal participation factor for Mode 1 is computed from the ratio  $L_1/M_1=2.206$ .

Table H-5  
Computation of Added Mass for the Inside Water Due to Ground Motion Along Transverse Direction (x-axis)

| Node No. | $Z_i$<br>m | Outside Geometry  |                   |                         | Equivalent Ellipse                |                           |                           | Equivalent Cylinder |                          | $m_a^i(z)$<br>$m_w^i$ | $m_a^i(z)$<br>MN-sec <sup>2</sup> /m <sup>2</sup> | $m_a^i(z)$<br>MN-sec <sup>2</sup> /m <sup>2</sup> |
|----------|------------|-------------------|-------------------|-------------------------|-----------------------------------|---------------------------|---------------------------|---------------------|--------------------------|-----------------------|---------------------------------------------------|---------------------------------------------------|
|          |            | $\frac{a_i}{b_i}$ | $\frac{a_i}{H_i}$ | $A_i$<br>m <sup>2</sup> | $\frac{\tilde{a}_i}{\tilde{b}_i}$ | $\frac{\tilde{a}_i}{H_i}$ | $\frac{\tilde{r}_i}{H_i}$ | $\frac{Z_i}{H_i}$   | $\frac{m_a^i(z)}{m_w^i}$ |                       |                                                   |                                                   |
| 1        | 2          | 3                 | 4                 | 5                       | 6                                 | 7                         | 8                         | 9                   | 10                       | 11                    | 12                                                |                                                   |
| 2        | 0          | 1.44              | 0.138             | 83.59                   | 1.44                              | 0.156                     | 0.109                     | 0.0                 | 1                        | 0.085                 | 0.085                                             |                                                   |
| 3        | 5.18       | 1.44              | 0.138             | 83.59                   | 1.44                              | 0.156                     | 0.109                     | 0.131               | 1                        | 0.085                 | 0.085                                             |                                                   |
| 4        | 10.97      | 1.44              | 0.138             | 83.59                   | 1.44                              | 0.156                     | 0.109                     | 0.277               | 1                        | 0.085                 | 0.085                                             |                                                   |
| 4'       | 10.97      | 1.48              | 0.142             | 85.95                   | 1.48                              | 0.161                     | 0.109                     | 0.277               | 1                        | 0.088                 | 0.088                                             |                                                   |
| 5        | 16.46      | 1.48              | 0.142             | 85.95                   | 1.48                              | 0.161                     | 0.109                     | 0.415               | 1                        | 0.088                 | 0.088                                             |                                                   |
| 6        | 22.56      | 1.48              | 0.142             | 85.95                   | 1.48                              | 0.161                     | 0.109                     | 0.569               | 1                        | 0.088                 | 0.088                                             |                                                   |
| 6'       | 22.56      | 1.52              | 0.146             | 88.24                   | 1.52                              | 0.165                     | 0.109                     | 0.569               | 1                        | 0.090                 | 0.090                                             |                                                   |
| 7        | 28.65      | 1.52              | 0.146             | 88.24                   | 1.52                              | 0.165                     | 0.109                     | 0.723               | 0.991                    | 0.090                 | 0.089                                             |                                                   |
| 8        | 34.75      | 1.52              | 0.146             | 88.24                   | 1.52                              | 0.165                     | 0.109                     | 0.877               | 0.894                    | 0.090                 | 0.080                                             |                                                   |
| 8'       | 34.75      | 1.56              | 0.150             | 90.68                   | 1.56                              | 0.169                     | 0.109                     | 0.877               | 0.894                    | 0.092                 | 0.082                                             |                                                   |
| 9        | 39.62      | 1.56              | 0.150             | 90.68                   | 1.56                              | 0.169                     | 0.109                     | 1                   | 0                        | 0.092                 | 0.000                                             |                                                   |

Note:

$$\frac{\tilde{a}_i}{H_i} = \frac{1}{H_i} \sqrt{\frac{A_i}{\pi} \left( \frac{a_i}{b_i} \right)}$$

(h) The maximum modal displacement is obtained from

$$Y_1 = \frac{L_1}{\omega_1^2} S_{al}(T_1, \xi_1) = \frac{2.206}{(12.467)^2} (1.289 \times 9.81 \times 1000) = 179 \text{ mm} \quad (\text{H-5})$$

(i) The maximum nodal displacements of the tower  $u_{jl}$  are obtained by multiplying  $Y_1$  computed in Step h by the mode shape  $\phi_{jl}$  in Column 2. The results are shown in Column 6.

(j) The Mode-1 elastic forces given by  $f_{jl} = \frac{L_1}{M_1} m_j \phi_{jn} S_{al}(T_1, \xi_1)$  are obtained by multiplying  $L_1/M_1$  (from Step g) and  $S_{al}$  (from Step b) by Column 4. The results are listed in Column 7.

(k) The shear force at each section along the tower height is obtained from the summation of elastic forces above that section  $V_{jl} = \sum_{k=j}^{13} f_{kl}$ . For example  $V_{13,1} = f_{13,1} = 2.427 \text{ MN}$ , and  $V_{12,1} = f_{12,1} + f_{13,1} = 2.427 + 7.152 = 9.579 \text{ MN}$ . The shear force at all nodal points is given in Column 8.

Table H-6  
Total Lumped Mass for Ground Motion Along Longitudinal axis (y-axis)

| Node No. | $m_o$ | $m_a^o$ | $m_a^i$ | $m_o + m_a^o + m_a^i$ | Length, m | $m_o + m_a^o + m_a^i$ | Total Mass at Point of Discontinuity |
|----------|-------|---------|---------|-----------------------|-----------|-----------------------|--------------------------------------|
| 1        | 0.524 | 0.241   |         | 0.765                 | 0.91      | 0.696                 |                                      |
| 2        | 0.524 | 0.241   |         | 0.765                 | 0.91      | 0.696                 | 2 + 2' =                             |
| 2'       | 0.199 | 0.152   | 0.085   | 0.436                 | 2.59      | 1.129                 | 1.825                                |
| 3        | 0.199 | 0.152   | 0.085   | 0.436                 | 5.18      | 2.258                 |                                      |
| 4        | 0.199 | 0.150   | 0.085   | 0.434                 | 2.59      | 1.124                 | 4 + 4' =                             |
| 4'       | 0.163 | 0.136   | 0.888   | 0.387                 | 3.05      | 1.180                 | 2.304                                |
| 5        | 0.163 | 0.133   | 0.088   | 0.384                 | 6.10      | 2.342                 |                                      |
| 6        | 0.163 | 0.127   | 0.087   | 0.377                 | 3.05      | 1.150                 | 6 + 6' =                             |
| 6'       | 0.129 | 0.115   | 0.089   | 0.333                 | 3.05      | 1.016                 | 2.166                                |
| 7        | 0.129 | 0.105   | 0.086   | 0.320                 | 6.10      | 1.952                 |                                      |
| 8        | 0.129 | 0.080   | 0.071   | 0.280                 | 3.05      | 0.854                 | 8 + 8' =                             |
| 8'       | 0.095 | 0.073   | 0.072   | 0.240                 | 2.44      | 0.586                 | 1.440                                |
| 9        | 0.095 | 0       | 0       | 0.095                 | 6.10      | 0.580                 |                                      |
| 10       | 0.095 |         |         | 0.095                 | 3.66      | 0.348                 | 10 + 10' =                           |
| 10'      | 0.063 |         |         | 0.063                 | 3.05      | 0.192                 | 0.540                                |
| 11       | 0.063 |         |         | 0.063                 | 5.79      | 0.365                 |                                      |
| 12       | 0.063 |         |         | 0.063                 | 2.74      | 0.173                 | 12 + 12' =                           |
| 12'      | 0.290 |         |         | 0.290                 | 0.30      | 0.087                 | 0.260                                |
| 13       | 0.290 |         |         | 0.290                 | 0.30      | 0.087                 |                                      |

(l) Finally the moment at each section is computed from multiplication of elastic forces acting above that section by their associated moment arms  $M_{j,l} = \sum_{k=j}^{13} h_k f_{kl}$ . For example  $M_{13,1} = 0 * 2.427 = 0.00 \text{ MN-m}$ , and  $M_{11,1} = 0 * 8.676 + 5.49 * 7.152 + 6.10 * 2.427 = 54.070 \text{ MN-m}$ . The results are given in Column 9.

The computation of Mode-2 response follows the same steps and is shown in Table H-10. The total response of the tower due to excitation along the transverse axis is then obtained by combining the Mode-1 and Mode-2 response quantities listed in Tables H-9 and H-10 by the simplified response spectrum analysis (SRSS) method. For example, the total response quantities at Node 10 are determined as follows:

$$u_{10} = \sqrt{u_{10,1}^2 + u_{10,2}^2} = \sqrt{129^2 + (-7)^2} = 129 \text{ mm} \quad (\text{H-6})$$

Table H-7  
Total Lumped Mass for Ground Motion Along Transverse Axis (x-axis)

| Node No. | $m_o$ | $m_a^o$ | $m_a^i$ | $m_o^+ + m_a^o + m_a^i$ | Length, ft | $m_o^+ + m_a^o + m_a^i$ | Total Mass at Point of Discontinuity |
|----------|-------|---------|---------|-------------------------|------------|-------------------------|--------------------------------------|
| 1        | 0.524 | 0.241   |         | 0.765                   | 0.91       | 0.696                   |                                      |
| 2        | 0.524 | 0.241   |         | 0.765                   | 0.91       | 0.696                   | 2 + 2' =                             |
| 2'       | 0.199 | 0.232   | 0.085   | 0.516                   | 2.59       | 1.336                   | 2.032                                |
| 3        | 0.199 | 0.231   | 0.085   | 0.515                   | 5.18       | 2.668                   |                                      |
| 4        | 0.199 | 0.228   | 0.085   | 0.512                   | 2.59       | 1.326                   | 4 + 4' =                             |
| 4'       | 0.163 | 0.219   | 0.088   | 0.470                   | 3.05       | 1.434                   | 2.760                                |
| 5        | 0.163 | 0.214   | 0.088   | 0.465                   | 6.10       | 2.836                   |                                      |
| 6        | 0.163 | 0.204   | 0.088   | 0.455                   | 3.05       | 1.388                   | 6 + 6' =                             |
| 6'       | 0.129 | 0.196   | 0.090   | 0.415                   | 3.05       | 1.266                   | 2.654                                |
| 7        | 0.129 | 0.180   | 0.089   | 0.398                   | 6.10       | 2.428                   |                                      |
| 8        | 0.129 | 0.134   | 0.080   | 0.343                   | 3.05       | 1.046                   | 8 + 8' =                             |
| 8'       | 0.095 | 0.129   | 0.082   | 0.306                   | 2.44       | 0.747                   | 1.793                                |
| 9        | 0.095 | 0.000   | 0.000   | 0.095                   | 6.10       | 0.580                   |                                      |
| 10       | 0.095 |         |         | 0.095                   | 3.66       | 0.348                   | 10 + 10' =                           |
| 10'      | 0.063 |         |         | 0.063                   | 3.05       | 0.192                   | 0.540                                |
| 11       | 0.063 |         |         | 0.063                   | 5.79       | 0.365                   |                                      |
| 12       | 0.063 |         |         | 0.063                   | 2.74       | 0.173                   | 12 + 12' =                           |
| 12'      | 0.290 |         |         | 0.290                   | 0.30       | 0.087                   | 0.260                                |
| 13       | 0.290 |         |         | 0.290                   | 0.30       | 0.087                   |                                      |

$$f_{10} = \sqrt{f_{10,1}^2 + f_{10,2}^2} = \sqrt{10.817^2 + (-5.360)^2} = 12.072 \text{ MN} \quad (\text{H-7})$$

$$V_{10} = \sqrt{V_{10,1}^2 + V_{10,2}^2} = \sqrt{29.072^2 + (-22.828)^2} = 36.964 \text{ MN} \quad (\text{H-8})$$

$$M_{10} = \sqrt{M_{10,1}^2 + M_{10,2}^2} = \sqrt{165.426^2 + (-164.920)^2} = 233.590 \text{ MN-m} \quad (\text{H-9})$$

The results for other nodes are given in Table H-11.

(2) Computer analysis. The results for computer response analysis using the SAP-IV program are displayed in Figures H-10 to H-12. Figure H-10 clearly demonstrates that the total displacements of the tower are due essentially to the first mode response and that the displacements for the third and higher modes are practically zero. Figure H-11 provides a comparison of shear forces for four different cases.

Table H-8  
Natural Periods of Vibration for Example Tower, sec

| Mode No. | Without Shear Deformation |              | With Shear Deformation |              |
|----------|---------------------------|--------------|------------------------|--------------|
|          | Transverse                | Longitudinal | Transverse             | Longitudinal |
| 1        | 0.4588                    | 0.3493       | 0.504                  | 0.388        |
| 2        | 0.1186                    | 0.0865       | 0.161                  | 0.124        |
| 3        | 0.0468                    | 0.0335       | 0.082                  | 0.063        |
| 4        | 0.0240                    | 0.0173       | 0.052                  | 0.041        |
| 5        | 0.0154                    | 0.0110       | 0.040                  | 0.032        |
| 6        | 0.0104                    | 0.0075       | 0.033                  | 0.026        |
| 7        | 0.0071                    | 0.0051       | 0.030                  | 0.023        |
| 8        | 0.0056                    | 0.0039       | 0.026                  | 0.021        |
| 9        | 0.0046                    | 0.0034       | 0.023                  | 0.019        |
| 10       | 0.0040                    | 0.0028       | 0.019                  | 0.015        |

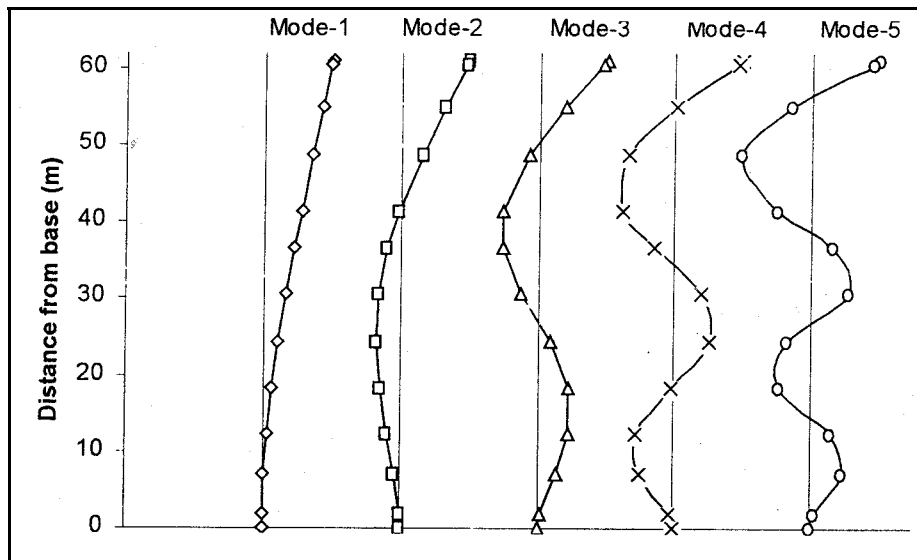


Figure H-9. Normalized lowest five mode shapes of example tower

The two-mode approximation of shear forces was computed manually in the previous paragraph, whereas those based on 10 modes of vibration were evaluated using SAP-IV. The computer analyses of shear forces were carried out for the standard and the site-specific ground motions with and without the effects of shear deformations. As expected, the shear forces for the standard response spectra are the largest, mainly because the standard response spectra show higher spectral accelerations than the site-specific spectra do (Figure H-2). The results also show that ignoring the effect of shear deformation would result

**Table H-9**  
**Mode-1 Nodal Displacements, Lateral Forces, Shears, and Overturning Moments Due to Ground Motion Along Transverse Axis (x-axis)**

| Node No. | $\phi_{j1}$ | $m_j$<br>MN-sec <sup>2</sup> /m <sup>2</sup> | $\phi_{j1} \times m_j$<br>MN-sec <sup>2</sup> /m <sup>2</sup> | $\phi_{j1}^2 \times m_j$<br>MN-sec <sup>2</sup> /m <sup>2</sup> | $u_{j1}$<br>mm | $f_{j1}$<br>MN | $V_{j1}$<br>MN | $M_{j1}$<br>MN |
|----------|-------------|----------------------------------------------|---------------------------------------------------------------|-----------------------------------------------------------------|----------------|----------------|----------------|----------------|
| 1        | 2           | 3                                            | 4                                                             | 5                                                               | 6              | 7              | 8              | 9              |
| 13       | 1.000       | 0.087                                        | 0.087                                                         | 0.087                                                           | 179            | 2.427          | 2.427          | 0.000          |
| 12       | 0.986       | 0.260                                        | 0.256                                                         | 0.253                                                           | 177            | 7.152          | 9.579          | 1.481          |
| 11       | 0.852       | 0.365                                        | 0.311                                                         | 0.265                                                           | 153            | 8.676          | 18.255         | 54.070         |
| 10       | 0.718       | 0.540                                        | 0.388                                                         | 0.278                                                           | 129            | 10.817         | 29.072         | 165.426        |
| 9        | 0.555       | 0.580                                        | 0.322                                                         | 0.179                                                           | 100            | 8.981          | 38.052         | 378.232        |
| 8        | 0.451       | 1.793                                        | 0.809                                                         | 0.365                                                           | 81             | 22.560         | 60.612         | 563.927        |
| 7        | 0.329       | 2.428                                        | 0.799                                                         | 0.263                                                           | 59             | 22.286         | 82.898         | 933.662        |
| 6        | 0.219       | 2.654                                        | 0.581                                                         | 0.127                                                           | 39             | 16.215         | 99.113         | 1439.338       |
| 5        | 0.128       | 2.836                                        | 0.363                                                         | 0.046                                                           | 23             | 10.127         | 109.240        | 2043.928       |
| 4        | 0.059       | 2.760                                        | 0.163                                                         | 0.010                                                           | 11             | 4.543          | 113.783        | 2710.295       |
| 3        | 0.020       | 2.668                                        | 0.053                                                         | 0.001                                                           | 4              | 1.489          | 115.272        | 3299.693       |
| 2        | 0.001       | 2.032                                        | 0.002                                                         | 0.000                                                           | 0              | 0.057          | 115.329        | 3896.802       |
| 1        | 0.000       | 0.696                                        | 0.000                                                         | 0.000                                                           | 0              | 0.000          | 115.329        | 4107.854       |

Note:  $L_1 = 4,134$   
 $M_1 = 1.874$   
 $L_1/M_1 = 2.206$   
 $S_a = 1.289$  g  
 $\omega = 12.467$  rad/sec

in 10 percent less base shear, but has negligible effect on the overturning moments. The two-mode approximation gives slightly smaller shear forces and overturning moments than the computer analysis, which considers 10 modes of vibration. The shears and moments due to the probabilistic seismic hazard analysis (PSHA) spectra are also smaller than those due to the standard spectra.

*c. Response due to longitudinal excitation.*

(1) Two-mode approximation. The two-mode approximation of the tower response due to excitation along the longitudinal axis is given in Tables H-12 to H-14. The computation steps are identical to those described in *b*(1) above, except that the periods, mode shapes, and the mass distribution associated with the vibration along the longitudinal axis of the tower are used. Again the Mode-1 (Table H-12) and Mode-2 responses (Table H-13) are computed separately and then combined using the SRSS method to obtain the total response due to the longitudinal excitation (Table H-14).

(2) Computer analysis. The results of computer response analysis for excitation along the longitudinal axis are given in Figures H-13 and H-14. The highest shear forces are obtained for the standard response spectra and the lowest shear forces for the case without shear deformation. The magnitudes of shear forces for the two-mode approximation and the 10-mode computer analysis are

Table H-10  
Mode-2 Nodal Displacements, Lateral Forces, Shears, and Overturning Moments Due to Ground Motion Along Transverse Axis (x-axis)

| Node No. | $\phi_{j2}$ | $m_j$<br>MN-sec <sup>2</sup> /m <sup>2</sup> | $\phi_{j2} \times m_j$<br>MN-sec <sup>2</sup> /m <sup>2</sup> | $\phi_{j2}^2 \times m_j$<br>MN-sec <sup>2</sup> /m <sup>2</sup> | $u_{j2}$<br>mm | $f_{j2}$<br>MN | $V_{j2}$<br>MN | $M_{j2}$<br>MN |
|----------|-------------|----------------------------------------------|---------------------------------------------------------------|-----------------------------------------------------------------|----------------|----------------|----------------|----------------|
| 1        | 2           | 3                                            | 4                                                             | 5                                                               | 6              | 7              | 8              | 9              |
| 13       | 1.000       | 0.087                                        | 0.087                                                         | 0.087                                                           | -20            | -2.657         | -2.657         | 0.000          |
| 12       | 0.967       | 0.260                                        | 0.251                                                         | 0.243                                                           | -19            | -7.678         | -10.335        | -1.621         |
| 11       | 0.640       | 0.365                                        | 0.234                                                         | 0.150                                                           | -13            | -7.134         | -17.469        | -58.360        |
| 10       | 0.325       | 0.540                                        | 0.176                                                         | 0.057                                                           | -7             | -5.360         | -22.828        | -164.920       |
| 9        | -0.006      | 0.580                                        | -0.003                                                        | 0.000                                                           | 0              | 0.106          | -22.722        | -332.025       |
| 8        | -0.170      | 1.793                                        | -0.305                                                        | 0.052                                                           | 3              | 9.309          | -13.414        | -442.909       |
| 7        | -0.287      | 2.428                                        | -0.697                                                        | 0.200                                                           | 6              | 21.281         | 7.867          | -524.732       |
| 6        | -0.308      | 2.654                                        | -0.817                                                        | 0.252                                                           | 6              | 24.964         | 32.831         | -476.743       |
| 5        | -0.252      | 2.836                                        | -0.715                                                        | 0.180                                                           | 5              | 21.825         | 54.656         | -276.477       |
| 4        | -0.151      | 2.760                                        | -0.417                                                        | 0.063                                                           | 3              | 12.727         | 67.393         | 56.924         |
| 3        | -0.067      | 2.668                                        | -0.179                                                        | 0.012                                                           | 1              | 5.459          | 72.842         | 405.969        |
| 2        | -0.006      | 2.032                                        | -0.012                                                        | 0.000                                                           | 0              | 0.372          | 73.215         | 783.293        |
| 1        | 0.000       | 0.696                                        | 0.000                                                         | 0.000                                                           | 0              | 0.000          | 73.215         | 917.276        |

Note:  $L_2 = -2.397$   
 $M_2 = 1.295$   
 $L_2/M_2 = -1.851$   
 $S_a = 1.682$  g  
 $\omega = 39.026$  rad/sec

essentially the same. The moments for the standard response spectra are the largest, but are about the same for the other three. The results indicate that the two-mode approximation method and shear deformation affect the shear forces more than they do the moments.

*d. Response due to transverse and longitudinal excitations.*

(1) The peak value of any resultant response quantity  $R$  due to the combined gravity and ground motion components is obtained from one of the following equations:

$$R = R_o \pm R_x \pm 0.5R_y \quad (\text{H-10})$$

$$R = R_o \pm 0.5R_x \pm R_y \quad (\text{H-11})$$

$$R = R_o \pm \sqrt{R_x^2 + R_y^2} \quad (\text{H-12})$$

**Table H-11**  
**Combined Mode-1 and Mode-2 Responses Due to 1000-year San Francisco Bay Area Ground Motion Applied Along Transverse Axis (x-axis)**

| <b>Node No.</b> | $u_j = \sqrt{u_{j1}^2 + u_{j2}^2}$<br><b>mm</b> | $f_j = \sqrt{f_{j1}^2 + f_{j2}^2}$<br><b>MN</b> | $V_j = \sqrt{V_{j1}^2 + V_{j2}^2}$<br><b>MN</b> | $M_j = \sqrt{M_{j1}^2 + M_{j2}^2}$<br><b>MN-m</b> |
|-----------------|-------------------------------------------------|-------------------------------------------------|-------------------------------------------------|---------------------------------------------------|
| 13              | 181                                             | 3.599                                           | 3.599                                           | 0.000                                             |
| 12              | 178                                             | 10.493                                          | 14.092                                          | 2.195                                             |
| 11              | 153                                             | 11.232                                          | 25.267                                          | 79.558                                            |
| 10              | 129                                             | 12.072                                          | 36.964                                          | 233.590                                           |
| 9               | 100                                             | 8.981                                           | 44.320                                          | 503.289                                           |
| 8               | 81                                              | 24.405                                          | 62.079                                          | 717.065                                           |
| 7               | 59                                              | 30.814                                          | 83.270                                          | 1071.013                                          |
| 6               | 40                                              | 29.768                                          | 104.409                                         | 1516.238                                          |
| 5               | 24                                              | 24.061                                          | 122.150                                         | 2062.543                                          |
| 4               | 11                                              | 13.514                                          | 132.239                                         | 2710.892                                          |
| 3               | 4                                               | 5.658                                           | 136.359                                         | 3324.573                                          |
| 2               | 0                                               | 0.377                                           | 136.606                                         | 3974.747                                          |
| 1               | 0                                               | 0.000                                           | 136.606                                         | 4209.021                                          |

where

$R_0$  = peak response due to gravity loads

$R_x$  = peak response due to the x-component of ground motion

$R_y$  = peak response due to the y-component of ground motion

Equations H-10 and H-11 are used with the standard response spectra, and Equation H-12 is employed with the site-specific response spectra. These equations are particularly applicable to the computation of section stresses.

(2) For the example tower with two axes of symmetry, gravity loads do not produce shears and moments. The x-component of ground motion produces shear only in the x-direction  $V_x$  and bending moment only about y-axis  $M_y$ . Similarly, the y-component of ground motion generates shear only in the y-direction  $V_y$  and bending moment only about the x-axis  $M_x$ . Therefore, for evaluation only the following combination of shears and moments need to be considered:  $V_x$  and  $0.5 V_y$ , with  $M_x$  and  $0.5 M_y$  and  $0.5 V_x$  and  $V_y$  with  $0.5 M_x$  and  $M_y$ .

(3) For the purpose of this example, the fault normal and the fault parallel components of ground motion response spectra (see paragraph 3-3b(4)) were assumed to be respectively 15 percent higher and 15 percent lower than the average equal-hazard spectra shown in Figure H-2. However, the standard response spectra were assumed to be the same for both horizontal directions. The combination of shear forces  $V_x$  and  $0.5V_y$  and bending moments  $M_x$  and  $0.5M_y$  for the site-specific and standard response spectra of ground motion are shown in Figures H-15 and H-16, respectively. The combination of shear forces  $0.5V_x$  and  $V_y$  and bending moments  $0.5M_x$  and  $M_y$  are presented in Figures H-17 and H-18, respectively.

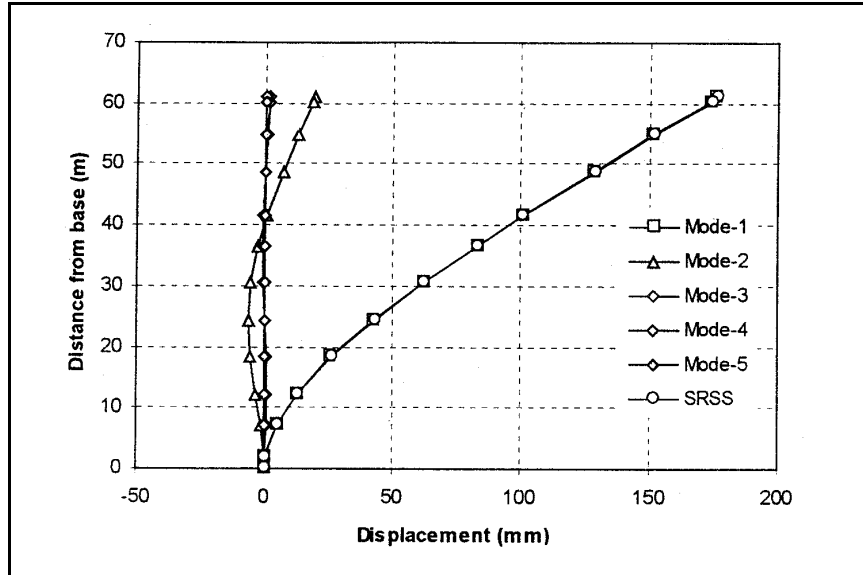


Figure H-10. Modal and SRSS displacements due to 1000-year San Francisco Bay area response spectra motion applied along x-axis (transverse direction)

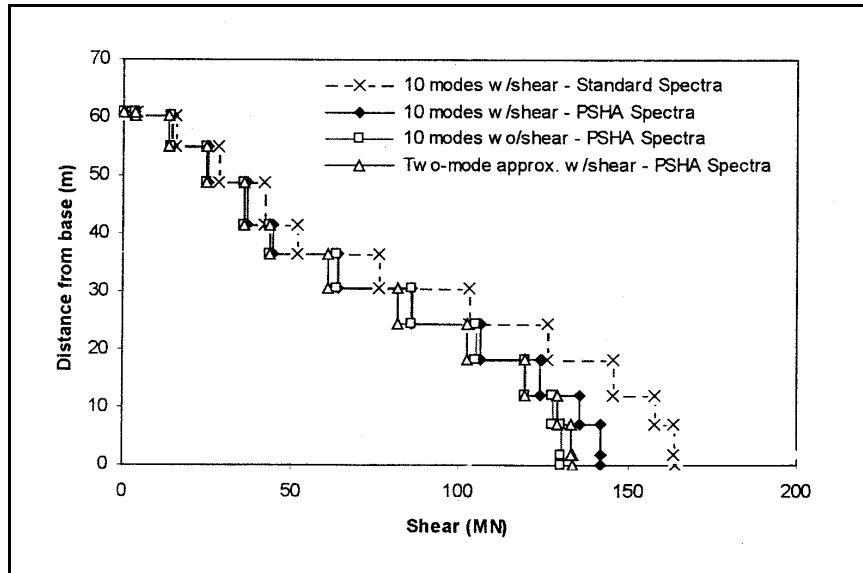


Figure H-11. Maximum shears due to 1000-year San Francisco Bay area response spectra applied along x-axis (transverse direction)

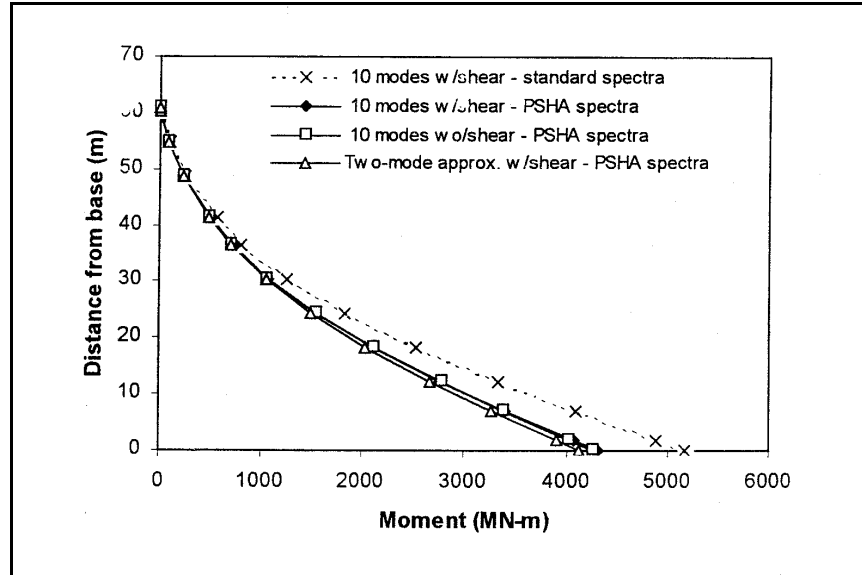


Figure H-12. Maximum moments due to 1000-year San Francisco Bay area response spectra applied along x-axis (transverse direction)

Table H-12  
Mode-1 Nodal Displacements, Lateral Forces, Shears, and Overturning Moments Due to Ground Motion Along Longitudinal Axis (y-axis)

| Node No. | $\phi_{j1}$ | $m_j$<br>MN-sec <sup>2</sup> /m <sup>2</sup> | $\phi_{j1} \times m_j$<br>MN-sec <sup>2</sup> /m <sup>2</sup> | $\phi_{j1}^2 \times m_j$<br>MN-sec <sup>2</sup> /m <sup>2</sup> | $u_{j1}$<br>mm | $f_{j1}$<br>MN | $V_{j1}$<br>MN | $M_{j1}$<br>MN |
|----------|-------------|----------------------------------------------|---------------------------------------------------------------|-----------------------------------------------------------------|----------------|----------------|----------------|----------------|
| 1        | 2           | 3                                            | 4                                                             | 5                                                               | 6              | 7              | 8              | 9              |
| 13       | 1.000       | 0.087                                        | 0.087                                                         | 0.087                                                           | 116            | 2.645          | 2.645          | 0.000          |
| 12       | 0.987       | 0.260                                        | 0.257                                                         | 0.253                                                           | 114            | 7.801          | 10.446         | 1.613          |
| 11       | 0.857       | 0.365                                        | 0.313                                                         | 0.268                                                           | 99             | 9.509          | 19.954         | 58.960         |
| 10       | 0.726       | 0.540                                        | 0.392                                                         | 0.285                                                           | 84             | 11.917         | 31.872         | 180.682        |
| 9        | 0.567       | 0.580                                        | 0.329                                                         | 0.186                                                           | 66             | 9.997          | 41.869         | 413.984        |
| 8        | 0.464       | 1.440                                        | 0.668                                                         | 0.310                                                           | 54             | 20.311         | 62.180         | 618.304        |
| 7        | 0.343       | 1.952                                        | 0.670                                                         | 0.230                                                           | 40             | 20.353         | 82.533         | 997.603        |
| 6        | 0.233       | 2.166                                        | 0.505                                                         | 0.118                                                           | 27             | 15.342         | 97.875         | 1501.054       |
| 5        | 0.140       | 2.342                                        | 0.328                                                         | 0.046                                                           | 16             | 9.967          | 107.842        | 2098.089       |
| 4        | 0.067       | 2.304                                        | 0.154                                                         | 0.010                                                           | 8              | 4.693          | 112.534        | 2755.924       |
| 3        | 0.025       | 2.258                                        | 0.056                                                         | 0.001                                                           | 3              | 1.716          | 114.250        | 3338.851       |
| 2        | 0.002       | 1.825                                        | 0.004                                                         | 0.000                                                           | 0              | 0.111          | 114.361        | 3930.668       |
| 1        | 0.000       | 0.696                                        | 0.000                                                         | 0.000                                                           | 0              | 0.000          | 114.361        | 4139.949       |

Note:  $L_1 = 3.762$   
 $M_1 = 1.794$   
 $L_1/M_1 = 2.097$   
 $S_a = 1.478$  g  
 $\omega = 16.194$  rad/sec

**Table H-13**  
**Mode-2 Nodal Displacements, Lateral Forces, Shears, and Overturning Moments Due to Ground Motion Along Longitudinal Axis (y-axis)**

| Node No. | $\phi_{j2}$ | $m_j$<br>MN-sec <sup>2</sup> /m <sup>2</sup> | $\phi_{j2} \times m_j$<br>MN-sec <sup>2</sup> /m <sup>2</sup> | $\phi_{j2}^2 \times m_j$<br>MN-sec <sup>2</sup> /m <sup>2</sup> | $u_{j2}$<br>mm | $f_{j2}$<br>MN | $V_{j2}$<br>MN | $M_{j2}$<br>MN |
|----------|-------------|----------------------------------------------|---------------------------------------------------------------|-----------------------------------------------------------------|----------------|----------------|----------------|----------------|
| 1        | 2           | 3                                            | 4                                                             | 5                                                               | 6              | 7              | 8              | 9              |
| 13       | 1.000       | 0.087                                        | 0.087                                                         | 0.087                                                           | -10            | -2.187         | -2.187         | 0.000          |
| 12       | 0.969       | 0.260                                        | 0.252                                                         | 0.244                                                           | -9             | -6.332         | -8.519         | -1.334         |
| 11       | 0.648       | 0.365                                        | 0.237                                                         | 0.153                                                           | -6             | -5.945         | -14.464        | -48.104        |
| 10       | 0.326       | 0.540                                        | 0.176                                                         | 0.057                                                           | -3             | -4.425         | -18.889        | -136.335       |
| 9        | -0.017      | 0.580                                        | -0.010                                                        | 0.000                                                           | 0              | 0.248          | -18.641        | -274.602       |
| 8        | -0.195      | 1.440                                        | -0.281                                                        | 0.055                                                           | 2              | 7.058          | -11.583        | -365.570       |
| 7        | -0.328      | 1.952                                        | -0.640                                                        | 0.210                                                           | 3              | 16.093         | 4.510          | -436.227       |
| 6        | -0.359      | 2.166                                        | -0.778                                                        | 0.279                                                           | 4              | 19.545         | 24.054         | -408.718       |
| 5        | -0.304      | 2.342                                        | -0.712                                                        | 0.216                                                           | 3              | 17.895         | 41.950         | -261.987       |
| 4        | -0.192      | 2.304                                        | -0.442                                                        | 0.085                                                           | 2              | 11.119         | 53.068         | -6.095         |
| 3        | -0.092      | 2.258                                        | -0.208                                                        | 0.019                                                           | 1              | 5.221          | 58.290         | 268.799        |
| 2        | -0.009      | 1.825                                        | -0.016                                                        | 0.000                                                           | 0              | 0.413          | 58.703         | 570.740        |
| 1        | 0.000       | 0.696                                        | 0.000                                                         | 0.000                                                           | 0              | 0.000          | 58.703         | 678.166        |

Note:  $L_2 = -2.336$   
 $M_2 = 1.407$   
 $L_2/M_2 = -1.661$   
 $S_a = 1.543$  g  
 $\omega = 50.671$  rad/sec

**Table H-14**  
**Combined Mode-1 and Mode-2 Responses Due to 1000-year San Francisco Bay Area Ground Motion Applied Along Longitudinal Axis (y-axis)**

| Node No. | $u_j = \sqrt{u_{j1}^2 + u_{j2}^2}$<br>mm | $f_j = \sqrt{f_{j1}^2 + f_{j2}^2}$<br>MN | $V_j = \sqrt{V_{j1}^2 + V_{j2}^2}$<br>MN | $M_j = \sqrt{M_{j1}^2 + M_{j2}^2}$<br>MN-m |
|----------|------------------------------------------|------------------------------------------|------------------------------------------|--------------------------------------------|
| 13       | 116                                      | 3.432                                    | 3.432                                    | 0.000                                      |
| 12       | 115                                      | 10.048                                   | 13.479                                   | 2.093                                      |
| 11       | 100                                      | 11.214                                   | 24.645                                   | 76.094                                     |
| 10       | 84                                       | 12.712                                   | 37.049                                   | 226.348                                    |
| 9        | 66                                       | 10.000                                   | 45.831                                   | 496.779                                    |
| 8        | 54                                       | 21.503                                   | 63.250                                   | 718.291                                    |
| 7        | 40                                       | 25.947                                   | 82.656                                   | 1,088.809                                  |
| 6        | 27                                       | 24.847                                   | 100.787                                  | 1,555.704                                  |
| 5        | 16                                       | 20.484                                   | 115.713                                  | 2,114.383                                  |
| 4        | 8                                        | 12.069                                   | 124.420                                  | 2,755.931                                  |
| 3        | 3                                        | 5.496                                    | 128.261                                  | 3,349.654                                  |
| 2        | 0                                        | 0.427                                    | 128.548                                  | 3,971.888                                  |
| 1        | 0                                        | 0.000                                    | 128.548                                  | 4,195.127                                  |

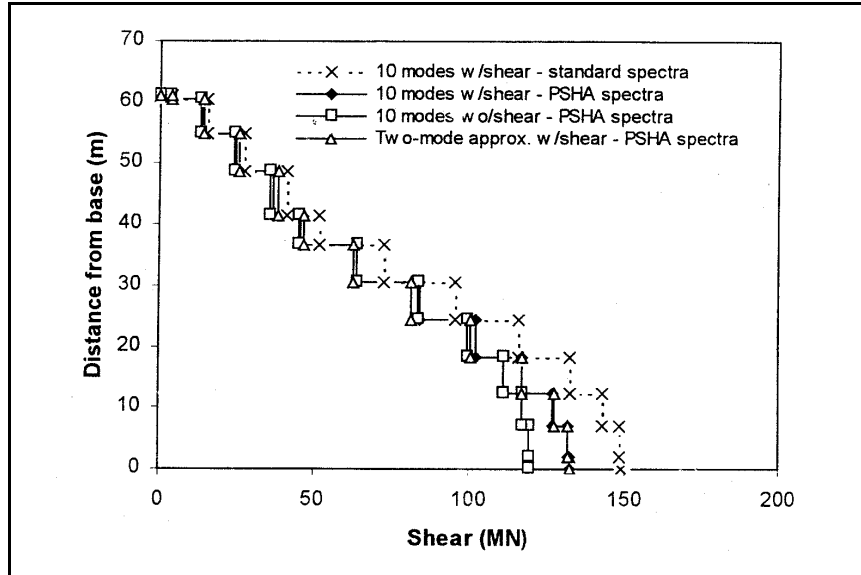


Figure H-13. Maximum shears due to 1000-year San Francisco Bay area response spectra applied along y-axis (longitudinal direction)

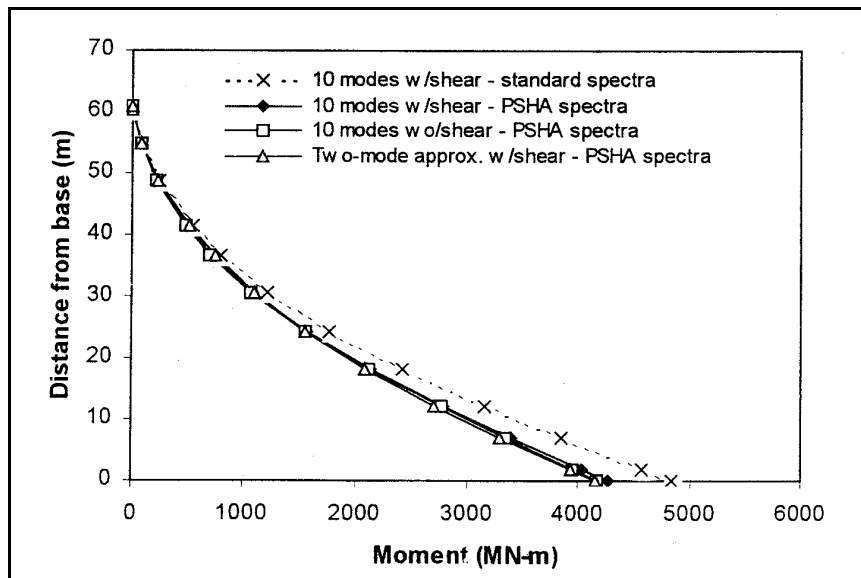


Figure H-14. Maximum moments due to 1000-year San Francisco Bay area response spectra applied along y-axis (longitudinal direction)

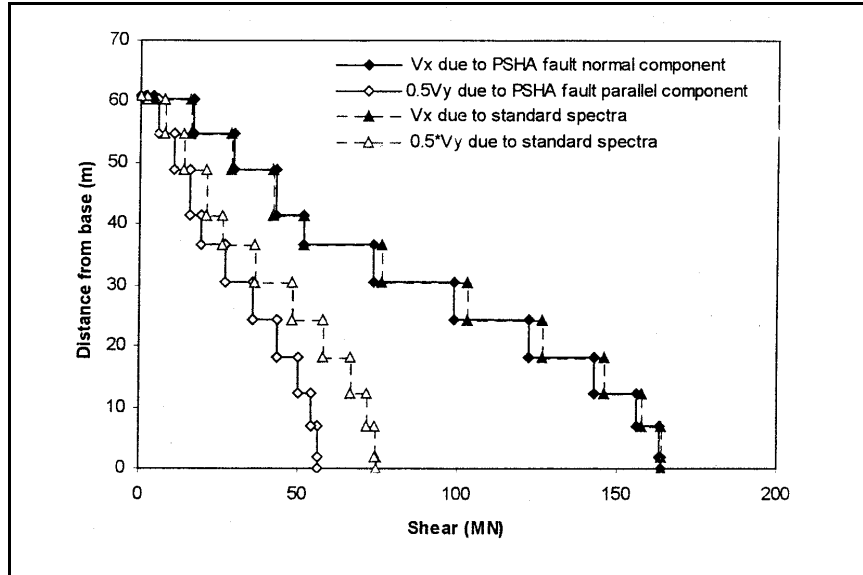


Figure H-15. Combination of shear forces  $V_x$  and  $0.5V_y$  for site-specific and standard ground motions

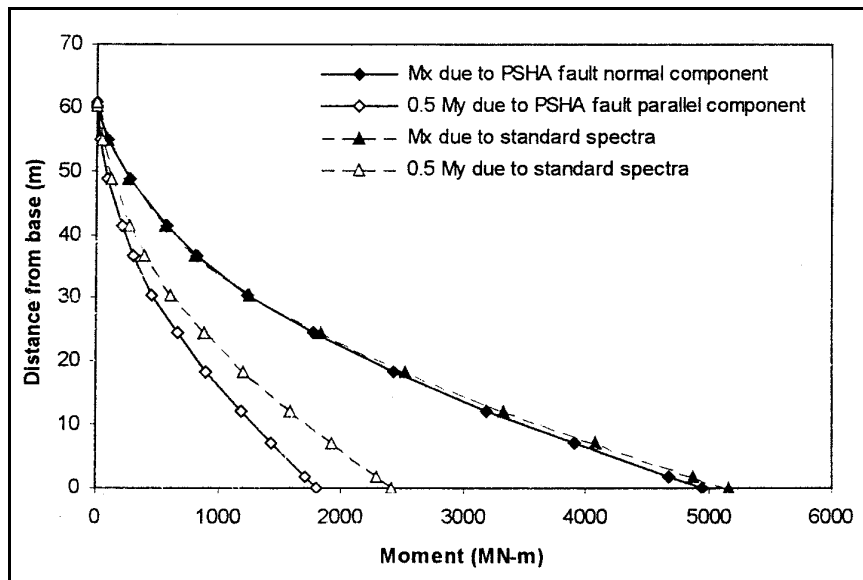


Figure H-16. Combination of moments  $M_x$  and  $0.5M_y$  for site-specific and standard ground motions

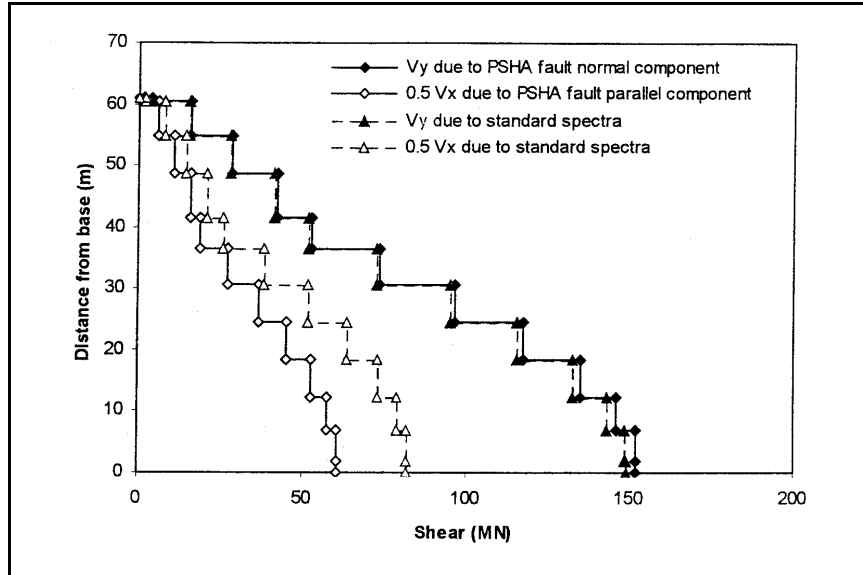


Figure H-17. Combination of shear forces  $0.5V_x$  and  $V_y$  for site-specific and standard ground motions

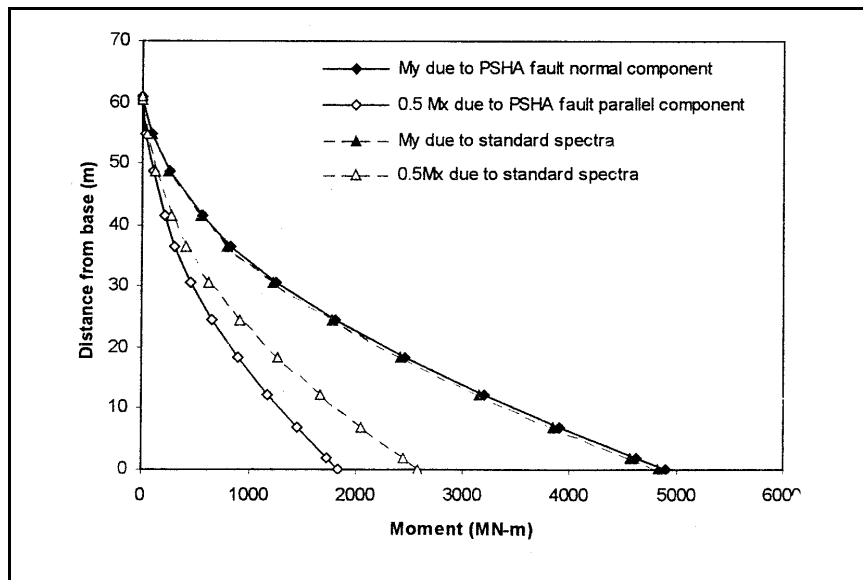


Figure H-18. Combination of shear forces  $0.5M_x$  and  $M_y$  for site-specific and standard ground motions

## H-7. Conversion Factors

| To Convert                          | Into                                | Multiply By |
|-------------------------------------|-------------------------------------|-------------|
| Meter (m)                           | ft                                  | 3.281       |
| m <sup>2</sup>                      | ft <sup>2</sup>                     | 10.764      |
| m <sup>4</sup>                      | ft <sup>4</sup>                     | 115.884     |
| Mega Newton (MN)                    | kip                                 | 224.81      |
| Mega Pascal (Mpa)                   | psi                                 | 145.038     |
| MN-m                                | kip-ft                              | 737.562     |
| MN-sec <sup>2</sup> /m              | k-sec <sup>2</sup> /ft              | 68.488      |
| MN-sec <sup>2</sup> /m <sup>2</sup> | k-sec <sup>2</sup> /ft <sup>2</sup> | 20.875      |
| MN/m <sup>3</sup>                   | pcf                                 | 6250        |